A Section 508–conformant HTML version of this article is available at https://doi.org/10.1289/EHP11600.

# Assessment of Nonalcoholic Fatty Liver Disease Symptoms and Gut–Liver Axis Status in Zebrafish after Exposure to Polystyrene Microplastics and Oxytetracycline, Alone and in Combination

*Weishang Zhou,[1]* Wei Shi,[1]* Xueying Du,[1] Yu Han,[1] Yu Tang,[1] Sanghyok Ri,[1,2] Kwangjin Ju,[1,3] Tongchol Kim,[1,2] Lin Huang,[1] Weixia Zhang,[1] Yihan Yu,[1] Dandan Tian,[1] Yingying Yu,[1] Liangbiao Chen,[4] Zhichao Wu,[4] and Guangxu Liu[1]*

[1]College of Animal Sciences, Zhejiang University, Hangzhou, P.R. China
[2]College of Life Science, Kim Hyong Jik University of Education, Pyongyang, DPR Korea
[3]College of Aquaculture, Wonsan Fisheries University, Wonsan, DPR Korea
[4]Key Laboratory of Exploration and Utilization of Aquatic Genetic Resources, Ministry of Education, Shanghai Ocean University, Shanghai, P.R. China

**Background:** Environmental pollution may give rise to the incidence and progression of nonalcoholic fatty liver disease (NAFLD), the most common cause for chronic severe liver lesions. Although knowledge of NAFLD pathogenesis is particularly important for the development of effective prevention, the relationship between NAFLD occurrence and exposure to emerging pollutants, such as microplastics (MPs) and antibiotic residues, awaits assessment.

**Objectives:** This study aimed to evaluate the toxicity of MPs and antibiotic residues related to NAFLD occurrence using the zebrafish model species.

**Methods:** Taking common polystyrene MPs and oxytetracycline (OTC) as representatives, typical NAFLD symptoms, including lipid accumulation, liver inflammation, and hepatic oxidative stress, were screened after 28-d exposure to environmentally realistic concentrations of MPs (0.69 mg/L) and antibiotic residue (3.00 μg/L). The impacts of MPs and OTC on gut health, the gut–liver axis, and hepatic lipid metabolism were also investigated to reveal potential affecting mechanisms underpinning the NAFLD symptoms observed.

**Results:** Compared with the control fish, zebrafish exposed to MPs and OTC exhibited significantly higher levels of lipid accumulation, triglycerides, and cholesterol contents, as well as inflammation, in conjunction with oxidative stress in their livers. In addition, a markedly smaller proportion of Proteobacteria and higher ratios of Firmicutes/Bacteroidetes were detected by microbiome analysis of gut contents in treated samples. After the exposures, the zebrafish also experienced intestinal oxidative injury and yielded significantly fewer numbers of goblet cells. Markedly higher levels of the intestinal bacteria-sourced endotoxin lipopolysaccharide (LPS) were also detected in serum. Animals treated with MPs and OTC exhibited higher expression levels of LPS binding receptor (*LBP*) and downstream inflammation-related genes while also exhibiting lower activity and gene expression of lipase. Furthermore, MP-OTC coexposure generally exerted more severe effects compared with single MP or OTC exposure.

**Discussion:** Our results suggested that exposure to MPs and OTC may disrupt the gut–liver axis and be associated with NAFLD occurrence. https://doi.org/10.1289/EHP11600

## Introduction

Nonalcoholic fatty liver disease (NAFLD), characterized by excessive fat accumulation in hepatocytes, was suggested to be the most common cause of chronic liver lesions.[1] Recent surveys have demonstrated that NAFLD is prevalent worldwide, specifically, ∼31.79%,[2] 30.45%,[2] and 27.37%[2] of the population in the Middle East, South America, and Asia, respectively, suffered from different degrees of NAFLD.[2–3] In addition, a significantly higher prevalence rate of NAFLD (i.e., up to 68.2% in obese children compared with 2.1% in normal children in China) was detected in obese individuals.[4–5] Considering the growing global epidemic of metabolic disorders, such as obesity, one group has predicted a 178% increase in liver-related deaths among individuals with NAFLD by 2030.[6–7] Therefore, with no effective and specific medication currently available for NAFLD, knowledge of NAFLD pathogenesis is particularly important for the development of effective prevention.

In recent years, accumulating data have suggested that exposure to environmental pollutants could be a tangible risk factor for NAFLD incidence and progression.[8–9] For example, it has been shown that exposure of mice to particulate matter ≤2.5 μm in aerodynamic diameter ($PM_{2.5}$) resulted in typical NAFLD symptoms, such as hepatic lipidosis, elevation of plasma triglycerides (TGs) and low-/very-low-density lipoproteins, and liver inflammation.[10] Similar NAFLD-inducing impacts have also been reported for a series of other environmental pollutants, such as thiamethoxam (TMX),[11] bisphenol A,[12] and 2,3,7,8-tetrachlorodibenzo-*p*-dioxin (TCDD).[13] However, the potential toxicity of many emerging pollutants known to be associated with the development of NAFLD, such as microplastics (MPs) and antibiotics, remains unknown.

Owing to the massive production[14] and use[15] of plastics in both industry and daily life (∼350–400 million tons of plastics are produced globally every year,[16] and the annual plastics consumption is predicted to surpass 1 billion tons by 2050[17]), plastic wastes are ubiquitously present in various environments, forming an emerging pollution phenomenon—plastic pollution.[18–19] Plastic pollution can be formed from the breakdown of larger pieces of plastic through weathering and biodegradation[20–21] or through the manufacture of small plastics *de novo*[22]; a large proportion of environmental plastics have a diameter of <5 mm and are collectively termed as MPs.[23–24] Humans may be exposed to environmental MPs through multiple routes,[25] for example, dermal contact,[26] inhalation,[27] and ingestion.[28] Recently, various types of MPs have been detected in different human tissues.[29–30] For instance, particles with sizes ≥700 nm of different types of plastics, including polystyrene (PS), polymethyl methacrylate

*These authors contributed equally to this work and are joint first authors of this manuscript.

Address correspondence to Guangxu Liu, College of Animal Sciences, Zhejiang University, 866 Yuhangtang Rd., Hangzhou, P.R. China 310058. Email: guangxu_liu@zju.edu.cn

Supplemental Material is available online (https://doi.org/10.1289/EHP11600).

The authors declare no competing interests.

Received 23 May 2022; Revised 31 October 2022; Accepted 23 February 2023; Published 7 April 2023.

**Note to readers with disabilities:** *EHP* strives to ensure that all journal content is accessible to all readers. However, some figures and Supplemental Material published in *EHP* articles may not conform to 508 standards due to the complexity of the information being presented. If you need assistance accessing journal content, please contact ehpsubmissions@niehs.nih.gov. Our staff will work with you to assess and meet your accessibility needs within 3 working days.

(PMMA), polypropylene (PP), polyethylene (PE), and polyethylene terephthalate (PET), were detected in whole blood samples collected from 22 healthy volunteers.[29] Similarly, a case study reported the detection of MPs (including PP and others that remained unidentified) with sizes ranging from 5 to 10 μm in the placenta of a pregnant woman.[30] Although drawing increasing public concern, the potential impact of MP exposure on individual health remains largely understudied.

In addition, characterized by their large specific surface area and hydrophobicity, MPs may adsorb other environmental pollutants, such as various antibiotics, through Van der Waals forces,[31] pore filling,[32] and electrostatic interaction.[33] For example, the Freundlich $K_f$ value was estimated to be $425 \pm 26$ $(mg/kg)(mg/L)^{1/n}$ for the absorption of oxytetracycline (OTC) on the surface of PS MPs.[32] In addition, indirect evidence (indicated by aggravated bioaccumulation of antibiotics in aquatic organisms in the co-presence of MPs) supporting antibiotics absorption on MPs surface was also increasingly documented.[34–35] Although adsorption capacities varied among pollutants, plastic types, and environmental conditions,[36] MPs may act as vectors for secondary pollutant internalization.[37] This highlights the need to investigate the health risks of MPs along with other common pollutants, such as antibiotics.

Since their discovery, antibiotics have been widely used ($\sim$34.8 billion daily defined doses in 2015[38]) for the treatment of diseases caused by pathogenic bacteria; however, massive application has led to the ubiquitous presence of antibiotic residues in various environments worldwide.[39–40] For example, it has been suggested that $\sim$30%–90% of OTC prescribed to patients failed to be degraded *in vivo* and ended up in the environment.[41] According to reports, the concentrations of OTC in soil, groundwater, and surface water can reach as high as 287 mg/kg (Southern China),[42] 237.0 ng/L (Southwestern China),[43] and 361.1 μg/L (Northern China),[44] respectively. Currently, in addition to consuming antibiotic-contaminated water and taking medically prescribed antibiotics, we are facing a severe risk of extra-dietary antibiotic (i.e., OTC) exposure. For instance, a significant amount of OTC residues has been found in milk (196.6–206.9 μg/L, India),[45] eggs (421.0–568.0 μg/kg, Nigeria),[46] honey (89.0–92.0 μg/kg, Turkey),[47] and seafood (2.7–8.6 μg/kg, USA).[48] With potential deleterious effects, such as gut microbiota dysbiosis, environmental antibiotic residues are widely regarded as a great threat to human health.[49]

Owing to the gut–liver axis, gut health has been shown to be closely related to that of the liver.[50–51] Previous case studies carried out in animal models (i.e., zebrafish[52] and mice[53]) have demonstrated that intestinal exposure to MPs and antibiotics may lead to microbiota dysbiosis and physiological damages. Although it has been stated in previous studies,[50,54] comprehensive and systematic investigations are urgently needed to assess the corresponding risk and detail the mechanisms of action where these effects have the potential to induce NAFLD through the gut–liver axis.

With the merits of high sequence homologies to humans and ease of manipulation, the zebrafish (*Danio rerio*) has been widely used as a model species to study NAFLD.[55–56] In the present study, the impacts of MPs and antibiotics (taking the commonly found environmental PS MPs and OTC as representatives) on the predisposition to NAFLD were assessed in zebrafish by screening typical NAFLD symptoms, including lipid accumulation (the size and abundance of lipid droplets, and lipid composition profiling of hepatocytes), liver inflammation (the content of pro-inflammatory cytokine and expressions of inflammation-related genes), and hepatic oxidative stress [*in vivo* content of reactive oxygen species (ROS), degree of lipid peroxidation, and activities of antioxidant enzymes]. In addition, gut health (the microbiome of gut contents, histomorphological characteristics, and oxidative injury), the level of the intestinal bacteria-sourced endotoxin lipopolysaccharide (LPS) in the circulatory system, as well as the gene expression of the endotoxin binding receptor in hepatocytes and the lipid catabolic activity of liver (activity of hepatic lipase and its gene expression) upon MP and OTC exposure were also evaluated to elucidate the potential mechanisms underlying NAFLD symptoms.

## Materials and Methods

### *Experimental Animals, Materials, and Chemicals*

Adult zebrafish (wild type, TU strain, 4 months old), commercial PS MPs (monosphere, diameter at $490 \pm 25$ nm; micrograph and physiochemical properties are provided in Figure S1 and Table S1), and standards of OTC (analytical grade, purity >95%) were purchased from FishBio Co., Ltd., Regal Nano-plastic Engineering Research Institute, and Solarbio Life Sciences (YZ130305), respectively. All experiments were approved by the animal care committee of Zhejiang University, and all methods were performed in accordance with the Guidelines for the Care and Use of Animals for Research and Teaching at Zhejiang University (ETHICS CODE permit no. ZJU20220031).

### *Exposure Experiments*

After acclimation in dechlorinated tap water (aeration for 72 h before use) for a week, zebrafish (480 individuals in total) were randomly assigned to four experimental groups (three replicates for each experimental group and 40 zebrafish for each replicate), namely, a control group, an MP-exposure group, an OTC-exposure group, and an MP-OTC coexposure group. According to previous studies, to simulate environmentally realistic pollution scenarios for fish species, 0.69 mg/L (equivalent to the MP level reported in the Miri River[57]) and 3.00 μg/L (equivalent to the average level of OTC reported in the Yangtze River and Tai Lakes[58]) were adopted as the exposure concentrations for MPs and OTC, respectively.

Exposure was conducted in tanks filled with 20 L of dechlorinated tap water containing the corresponding designated concentrations. Water was filtered through a 0.45-μm membrane filter before use to minimize potential waterborne MP contamination. During the 28-d exposure, the temperature and pH of the experimental water were maintained at $28.0 \pm 0.5^{\circ}C$ and $7.1 \pm 0.2$, respectively; in addition, a light cycle of 14-h light/10-h dark was adopted. Commercial food pellets (FishBio Co., Ltd.) were provided and the experimental water was renewed daily after feeding. After corresponding exposure, the zebrafish were anesthetized in 0.02% tricaine (E10521; Sigma-Aldrich) and sacrificed in ice water before obtaining the tissue specimens.

Following reported methods, the background and working concentrations of MPs and OTC in each exposure group (Table S2) were determined using high-performance liquid chromatography–mass spectrometry (HPLC/MS)[59] and light microscopy,[60] respectively. Briefly, 1 L of water sampled from each experimental tank was filtered through a 0.7-μm glass fiber filter (GF/F; Whatman), acidified to pH 3.0 with 40% sulfuric acid (vol/vol), and then transferred into an activated solid-phase extraction column (HLB; 6 mL, 500 mg; Waters). After methanol elution and evaporation, pure water was added to the sample to a final volume of 1.0 mL. The OTC concentration in the sample was then determined by HPLC/MS (TSQ Quantum; Thermo Scientific) at the detection limit of 11.43 ng/L. To quantify the concentration of MPs in water, 10 μL of water was sampled from each experimental tank and the number of MPs in the sample was determined under a microscope

(BX53; Olympus) with a hemocytometer at the magnification of 1,000×.

To verify the interactions between MPs and OTC in the experimental medium, the absorption of OTC on surface of the MPs and the effect of OTC on MP dispersing characteristics were determined with Fourier infrared spectroscopic (FT-IR) analysis[61] and dynamic light scattering measurement,[62] respectively (Figures S2–S4). In brief, MP water samples with and without OTC were injected into a closed liquid pool with a thickness of 1 mm, and the transmittance of samples were measured with a FT-IR spectrometer (NICOLET iS50FT-IR; Thermo Scientific) in the wavenumber range of 4,000–400/cm. The particle size and zeta potential of MPs in water with and without OTC were determined with a Zetasizer (Nano ZS90; Malvern) at 25°C at the detection angle of 173° with a red laser (633 nm, 4 mW) and an avalanche photodiode detector (quantum efficiency >50% at 633 nm). In this measurement, the attenuator position was set at 4.65 mm and the attenuation speed was set to be automatically based on the size and concentration of the MPs.

### *Histological Observation and Biochemical Profiling of Lipids in the Liver*

Following methods previously reported,[63] lipid accumulation in zebrafish livers was assessed microscopically using Oil Red O staining. Briefly, after the corresponding exposure, hepatic tissues dissected from six individuals in each experimental group ($n=6$) were fixed with 4% paraformaldehyde, washed with phosphate-buffered saline (PBS), dehydrated with sucrose solution for 6 h, and then preserved at −80°C individually. Tissue samples were embedded in optimal cutting temperature compound (OCT; 4583; SAKURA), cryosectioned into 16-μm sections using a cryostat microtome (CM 1950; Leica), and subsequently stained with Oil Red O (0.5 mg Oil Red in 100 mL anhydrous isopropyl alcohol and then diluted with 40% distilled water) according to standard procedures. In brief, frozen sections were washed with distilled water to remove redundant OCT and steeped with 60% isopropyl alcohol for 2 min, followed by incubation in Oil Red O solution for 5 min. After immediate rinsing with running water, samples were stained with hematoxylin for 2 min, differentiated with 1% alcohol hydrochloride for 2 s, and then washed again with distilled water. Once sealed with glycerin gelatin, the size and abundance of lipid droplets accumulated in the hepatic tissue were examined under a light microscope (Eclipse Ci-L; Nikon).

The triglyceride (TG), total cholesterol (TCHO), free fatty acid (FFA), and total bile acid (TBA) levels in zebrafish livers were determined using the corresponding commercial kits [BC0625, BC1985, and BC0595 (Solarbio) and E003-2-1 (Njjcbio), respectively].[64] Briefly, livers dissected from three individuals from the same replicate of an experimental group were pooled as one sample [18 individuals and six samples ($n=6$) in total for each experimental group] with each parameter investigated to meet the quantity requirements of analysis. After homogenization and the addition of the extraction solution provided in kit, the sample was immediately centrifuged at 4°C for 10 min. The color development reaction was then conducted by mixing the supernatant collected with the corresponding chromogenic reagent, following the manufacturer's instructions. The absorption values of the supernatants (wavelengths at 420, 500, 550, and 405 nm for TGs, TCHO, FFAs, and TBAs, respectively) were determined using a microplate reader (Multiskan GO; Thermo Scientific). After protein content quantification using the Bradford method (P0006; Beyotime),[65] the contents of TG, TCHO, FFA, and TBA in zebrafish livers were calculated using the absorption values obtained and expressed as micromoles per milligram of protein.

### *Assessment of Hepatic Inflammation*

The expression levels of four classic inflammation-related genes, including myeloid differentiation primary response 88 (*MyD88*), tumor necrosis factor (TNF) receptor–associated factor 6 (*TRAF6*), nuclear factor kappa-light-chain-enhancer of activated B cells p105 subunit (*NFκB*), and *TNF-α*, in zebrafish livers after the corresponding exposures were assessed using real-time polymerase chain reaction (PCR). Nine zebrafish were selected from each experimental group, and the livers of three individuals from the same replicate were pooled as one sample ($n=3$ for each experimental group). After RNA extraction with the EASYspin Plus RNA extraction kit (RN2802; Aidlab) and complementary DNA (cDNA) generation with PrimeScript RT Reagent (RR037A; TaKaRa), real-time PCR was performed with a Bio-Rad real-time system (CFX96; Bio-Rad) using the following program: initial denaturation at 95°C for 5 min, followed by 40 cycles of 95°C for 10 s, 60°C for 30 s, and 72°C for 30 s, and a final step of 72°C for 5 min. β-actin was used as the internal reference, and all primer information (including both sequence and accession number of corresponding gene) are provided in Table S3. All PCR primers were synthesized by Tsingke Biotechnology Co., Ltd., and relative expression levels were analyzed using the $2^{-\Delta\Delta CT}$ method.[66]

Hepatic inflammation status of zebrafish after the corresponding 28-d treatments was further evaluated by quantifying TNF-α, a pro-inflammatory cytokine, using western blotting.[67] Three individuals were selected from each experimental group (one individual from each replicate tank and $n=3$ for each experimental group) and dissected on ice. Fresh individual liver tissue was homogenized and mixed with commercial radioimmunoprecipitation assay buffer (P0013B; Beyotime) supplemented with the protease inhibitor phenylmethylsulfonyl fluoride (ST506; Beyotime) and 1× complete (11697498001; Roche), followed by centrifugation at 13,800× *g* at 4°C for 15 min. After protein content determination as described above, the collected supernatant was mixed with sodium dodecyl sulfate (SDS) buffer (total protein/SDS = 1:2), heated at 100°C for 5 min, separated on a 10% SDS–polyacrylamide gel electrophoresis system, and then electrotransferred onto a polyvinylidene fluoride membrane. The membrane was blocked with QuickBlock Western Occluder (P0252; Beyotime) at room temperature for 4 h and then immunoblotted overnight at 4°C with the primary antibodies TNF-α (1:500) and β-actin (1:1,000) (R1203-1 and R1207-1, respectively; HuaBio). After incubation with horseradish peroxide (HRP)–conjugated goat anti-rabbit immunoglobulin G (1:2,000) (HA1001; HuaBio) and exposure with a gel imager (ClinxChemiScope 3400; Clinx), TNF-α expression levels were determined using ImageJ software.[68]

### *Evaluation of Oxidative Stress in the Livers*

After corresponding exposures, the *in vivo* ROS content in hepatic tissue was determined *in situ* using ROS-specific fluorescent staining.[69] Following the method described above, cryosections (20-μm thick) were prepared from fresh hepatic tissues collected individually from six zebrafish in each experimental group (2 individuals from each replicate and $n=6$ for each experimental group). After staining with ROS-specific fluorescent dihydroethidium [DHE; dissolved in dimethyl sulfoxide (DMSO) to 2 mg/mL and diluted with PBS at a ratio of 1:500] dye (D7008; Sigma) at 37°C for 30 min and three rounds of PBS washes on a decolorizing shaker (5 min each), samples were incubated with 4′,6-diamidino-2-phenylindole (DAPI; D9542; Sigma) in the dark at room temperature for 10 min. Images were then captured using a fluorescence microscope

(Eclipse E100; Nikon) at excitation and emission wavelengths of 535 and 610 nm, respectively. The ROS-specific fluorescence intensity of each sample was subsequently determined using ImageJ software, according to the method reported.[70]

The degree of lipid peroxidation indicated by the content of its terminal product, malondialdehyde (MDA), and the activities of two antioxidant enzymes, superoxide dismutase (SOD) and catalase (CAT), in zebrafish livers were measured using the corresponding commercial kits (BC0025, BC0175, and BC0205, respectively; Solarbio). For each parameter investigated, 18 individuals were selected from each experimental group (6 of each replicate), and the livers from 3 zebrafish were pooled as one sample ($n = 6$ in total for each experimental group). Following the protocols reported in our previous study,[71] pooled samples were homogenized on ice with the extraction solution provided. The supernatant was collected by centrifugation at $8{,}000 \times g$ and 4°C for 10 min and used to determine the MDA content and SOD and CAT activities. For MDA content estimation, the supernatant was mixed with thiobarbituric acid at 100°C for an hour followed by centrifugation at $10{,}000 \times g$ for 10 min. The absorption values at three wavelengths (450, 532, and 600 nm) were then recorded with a microplate reader (Multiskan GO; Thermo Scientific). For SOD and CAT enzymatic activities, supernatant was mixed with the corresponding reaction solution (nitro-blue tetrazolium and hydrogen peroxide for SOD and CAT, respectively) for 30 min at 37°C. The absorption value was then determined at 560 and 240 nm for SOD and CAT, respectively. After protein content determination as described above, the MDA content and the SOD and CAT activities in the sample were calculated with the absorption values obtained following the manufacturer's instructions and standardized with the protein content of the sample.

### *Microbiome Analysis of Gut Contents*

After a 28-d exposure and a 24-h fasting period, the intestines were dissected individually from 18 zebrafish for each experimental group (6 individuals from each replicate), and the gut contents squeezed out from the 6 individuals from the same replicate were pooled as one sample ($n = 3$ for each experimental group) to meet the minimum amount required for analysis. Total genomic DNA of each sample was then extracted using the cetyltrimethylammonium bromide (CTAB) method according to the reported protocol.[72] Briefly, samples were incubated with CTAB lysis buffer [100 mM Tris-hydrochloride, 100 mM ethylenediaminetetraacetic acid (EDTA), 100 mM sodium phosphate, 1.5 M sodium chloride, 1% CTAB] and protease K (10 mg/mL) for 30 min at 37°C. After protease treatment and adding phenol/chloroform/isoamyl alcohol (vol:vol:vol, 25:24:1) solution, the sample was centrifuged at $12{,}000 \times g$ for 10 min. Chloroform/isoamyl alcohol (vol:vol, 24:1) was then added to the obtained supernatant, followed by centrifugation at $12{,}000 \times g$ for 10 min. Isoamyl alcohol was subsequently added to the obtained supernatant to precipitate DNA. After purification with 75% ethyl alcohol and RNA removal using RNase solution, the DNA sample was collected by centrifugation ($12{,}000 \times g$ for 10 min) and dissolved in double-distilled water, followed by quality verification and quantity determination using electrophoresis (1% agarose gel) and a NanoDrop spectrophotometer (Thermo Scientific), respectively. The hypervariable region V4 of the bacterial 16S rRNA was amplified using specific primers 515F (5′-GTGCCAGCMGCCGCGGTAA-3′) and 806R (5′-GGACTACHVGGGTWTCTAAT-3′) obtained from the Novogene Co., Ltd. Amplification was carried out in 15 μL of Phusion High-Fidelity PCR Master Mix (New England Biolabs) containing 2 μM of forward and reverse primers and 10 ng of template DNA using the following thermal cycles: initial denaturation at 98°C for 1 min, followed by 30 cycles of denaturation at 98°C for 10 s, annealing at 50°C for 30 s, and elongation at 72°C for 30 s, and a final step at 72°C for 5 min. The purified PCR products were then subjected to Illumina-based high-throughput sequencing (Novogene Co., Ltd.). The obtained sequencing data were submitted to the National Center for Biotechnology Information (NCBI) database under the accession number of PRJNA890774.

According to methods reported previously,[73] after removing chimeric sequences, Uparse software (version 7.0.1001) was used to analyze the sequences obtained. Sequences with ≥97% similarity were assigned to the same operational taxonomic units (OTUs), and a representative sequence for each OTU was screened for further annotation using the Silva database. OTU abundance information was normalized using a standard sequence number corresponding to the sample with the least sequences. The Firmicutes/Bacteroidetes ratio (F/B ratio), a key indicator for obesity in both human[74] and fish[75] according to previous studies, was then calculated based on the corresponding abundance obtained.

### *Histopathological Examination and Oxidative Injury of the Intestines*

Following the methods reported,[76] intestines dissected individually from six zebrafish in each experimental group (2 individuals from each replicate and $n = 6$ for each experimental group) were fixed with 4% paraformaldehyde for 24 h, dehydrated with ethanol (75%, 85%, 95%, and 100% ethanol, sequentially), transparentized with xylene solution, embedded in paraffin wax, and then transversely sliced into 5-μm sections with a rotary microtome (RM2016; Leica). After dewaxing and rehydration, the samples were stained with hematoxylin for 5 min and then differentiated with 0.1% hydrochloric acid ethanol. After removing extra hematoxylin with distilled water, the sample was stained with eosin for 3 min. The stained sample was dehydrated with ethanol as described above and then sealed with glycerin gelatin. After the abovementioned hematoxylin and eosin (H&E) staining, the sample was examined microscopically (Eclipse Ci-L; Nikon). The number of intestinal goblet cells, an important indicator of the intestinal barrier in zebrafish according to previous studies,[76–77] was determined and used to calculate their density in the observed area.

After the corresponding 28-d exposure, intestines were dissected individually from six zebrafish in each experimental group (2 individuals from each replicate and $n = 6$ for each experimental group) to estimate the intestinal accumulation of OTC and degree of oxidative damage. Following the methods reported in our previous study,[34] the OTC concentrations in zebrafish intestines (Figure S5) were determined using HPLC/MS. Briefly, after EDTA–McIlvaine (0.1 M) ultrasonic extraction at 4°C for 30 min and centrifugation at $900 \times g$ for 5 min, the supernatant collected from the intestine sample was transferred into an HLB solid-phase extraction column, followed by elution with methanol and ethyl acetate. The eluate was collected, dried with nitrogen, and then redissolved in 1 mL of methanol/trifluoroacetic acid mixture (vol:vol, 1:19). After filtration through a 0.45-μm membrane, the amount of OTC in the sample was determined by HPLC-MS (ACQUITY I-Class/Xevo TQ-S; Waters). According to the methods described in the section "Evaluation of Oxidative Stress in the Livers," the level of oxidative injury was estimated by measuring the MDA content in the intestines. In brief, after incubating the supernatant collected from the homogenized sample with thiobarbituric acid at 100°C for an hour, the absorption values (at 450, 532, and 600 nm) of the sample were determined with a microplate reader (Multiskan GO; Thermo Scientific). The MDA content in the sample was subsequently calculated with the absorption values obtained following the manufacturer's instructions and standardized with the protein content of the sample.

### *Quantification of LPS Content in Serum and Expression Analysis of Its Receptor in Hepatocytes*

Following the reported methods,[78] the content of bacteria-sourced endotoxin LPS in zebrafish serum was measured using a commercial LPS enzyme-linked immunosorbent assay kit (JL13861; Jonln Biotechnology). To obtain sufficient serum for analysis, 54 zebrafish were used from each experimental group (18 individuals from each replicate) and blood extracts from 9 individuals from the same replicate were pooled as one sample ($n = 6$ for each experimental group in total). After clotting at 4°C overnight and centrifugation at $1,000 \times g$ for 20 min, the obtained supernatant (serum) was incubated with HRP-labeled antibodies at 37°C for an hour, followed by 15 min of incubation (37°C) with the chromogenic reagent provided. Upon adding the stop solution, the absorption value of each sample was measured at a wavelength of 450 nm using a microplate reader (Multiskan GO; Thermo Scientific). After quantifying the protein content of each sample as described above, the LPS content in the serum was calculated using the absorption value obtained and standardized with the protein content following the manufacturer's instructions.

Following methods described in the section "Assessment of Hepatic Inflammation," the gene expression of LPS binding protein (*LBP*) in zebrafish liver ($n = 3$ for each experimental group) after corresponding exposures was analyzed by real-time PCR using β-actin as an internal reference. Briefly, after RNA extraction with the EASYspin Plus RNA extraction kit (RN2802; Aidlab) and cDNA generation with PrimeScript RT Reagent (RR037A; TaKaRa), real-time PCR was performed with a Bio-Rad real-time system (CFX96; Bio-Rad) using the amplification program described in section "Assessment of Hepatic Inflammation" and primers described in Table S3.

### *Determination of Lipase Activity and Its Gene Expression in the Liver*

After the corresponding 28-d treatments, the lipase activity in the zebrafish livers was determined using a commercial lipase activity kit (BC2345; Solarbio) following the methods previously reported.[79] Eighteen zebrafish were selected from each experimental group (6 individuals from each replicate) and the livers of 3 individuals from the sample replicate were pooled as one sample ($n = 6$ for each experimental group). After homogenization on ice and centrifugation at 4°C ($12,000 \times g$), the obtained supernatant was fully mixed with the reaction substrate (olive oil) at 37°C for 10 min. Once the decomposition reaction was terminated by the provided stop solution, the sample was fully mixed with copper sulfate solution for color development. The absorbance value of each supernatant obtained was then determined at 710 nm with a microplate reader (Multiskan GO; Thermo Scientific) and used to calculate the lipase activity of the sample, following the manufacturer's instructions. One unit of lipase activity was defined as the amount of lipase that catalyzes the release of 1 μmol of FFAs from olive oil per milligram of protein per minute at 37°C.

In addition, expression level of the gene encoding lipase (*LIP*) in the zebrafish liver (1 individual collected from each replicate and $n = 3$ for each experimental group) after the corresponding 28-d treatments was analyzed by real-time PCR following the same method described above. Primers used for *LIP* expression analysis are listed in Table S3.

### *Statistical Analysis*

All parameters were compared among the different experimental groups using one-way analysis of variance and Tukey's post hoc tests after verification of data normality and variance homogeneity with the Shapiro–Wilk test and Levene's test, respectively. All analyses were conducted using OriginPro (version 8.0), and statistical significance was set at $p < 0.05$.

## Results

### *Hepatic Lipid Accumulation in Zebrafish*

Compared with control, lipid-specific Oil Red O staining results (Figure 1) demonstrated that zebrafish exposed to MPs, OTC, and MP-OTC exhibited more (Figure 1B; $F_{3,8} = 41.28$, $p < 0.05$) and larger (Figure 1C; $F_{3,8} = 60.11$, $p < 0.05$) lipid droplets (Lds) accumulated in their livers. In addition, markedly higher TG (Figure 2A; $F_{3,20} = 38.69$, $p < 0.05$) and TCHO (Figure 2B; $F_{3,20} = 18.24$, $p < 0.05$) contents, whereas lower FFA (Figure 2C; $F_{3,20} = 34.40$, $p < 0.05$) and TBA (Figure 2D; $F_{3,20} = 95.57$, $p < 0.05$) contents were observed in the liver samples treated with MPs, OTC, and MP-OTC. Among all experimental groups, the most and largest Lds, the highest TG and TCHO contents, and the least FFA and TBA contents were detected in MP-OTC coexposed samples (Figures 1 and 2).

### *Status of Hepatic Inflammation*

Compared with the control fish, the zebrafish treated with MPs, OTC, and MP-OTC yielded significantly higher expression levels of the four classic inflammation-related genes *MyD88*, *TRAF6*, *NFκB*, and *TNF-α* in their livers (Figure 3A). Similarly, markedly higher levels of pro-inflammatory cytokine (TNF-α) were detected by western blotting in samples exposed to MPs, OTC, and MP-OTC and which were ∼1.20, 1.42, and 1.65 times that of the control, respectively (Figure 3B; $F_{3,8} = 27.19$, $p < 0.05$). In addition, compared with those treated with MPs or OTC alone, animals coexposed to MPs and OTC showed significantly higher expression levels of the inflammation-related genes tested and TNF-α (Figure 3).

### *Status of Oxidative Stress in Liver*

DHE staining (Figure 4) demonstrated that zebrafish exposed to MPs, OTC, and MP-OTC for 28 d had significantly higher ROS-specific fluorescent intensity in their livers, ∼2.40, 3.29, and 4.23 times that of the control, respectively (Figure 4B; $F_{3,20} = 133.52$, $p < 0.01$). Similarly, compared with the control, higher levels of MDA content were detected in MPs, OTC, and MP-OTC groups, ∼1.77, 2.12, and 2.46 times that of the control, respectively (Figure 4C; $F_{3,20} = 39.61$, $p < 0.05$). In addition, significantly lower SOD activity was observed in MPs, OTC, and MP-OTC samples, ∼65.50%, 63.55%, and 31.96% of that of the control, respectively (Figure 5A; $F_{3,20} = 17.14$, $p < 0.05$). Zebrafish of the OTC- and the MP-OTC–exposure groups also exhibited lower CAT activity in their livers, ∼96.61% and 84.40% of that of the control, respectively (Figure 5B; $F_{3,20} = 108.34$, $p < 0.05$). Finally, zebrafish coexposed to MPs and OTC were shown to have markedly higher ROS-specific fluorescent intensity and MDA content, but lower activities of SOD and CAT compared with those singly treated with MPs or OTC (Figures 4 and 5).

### *Microbiome of Gut Contents*

Significant differences in microbiome composition among the experimental groups were detected in the gut contents by sequencing analysis (Figure 6). At the phylum level, Proteobacteria was the most abundant microbial found in the gut contents of zebrafish and accounted for ∼81.45%, 78.73%, 68.91%, and 76.48% for the control, MP, OTC, and MP-OTC groups, respectively (Figure 6A). In addition, zebrafish exposed to MPs, OTC, and MP-OTC gave higher F/B ratios, ∼6.85%, 8.82, and 9.68 times

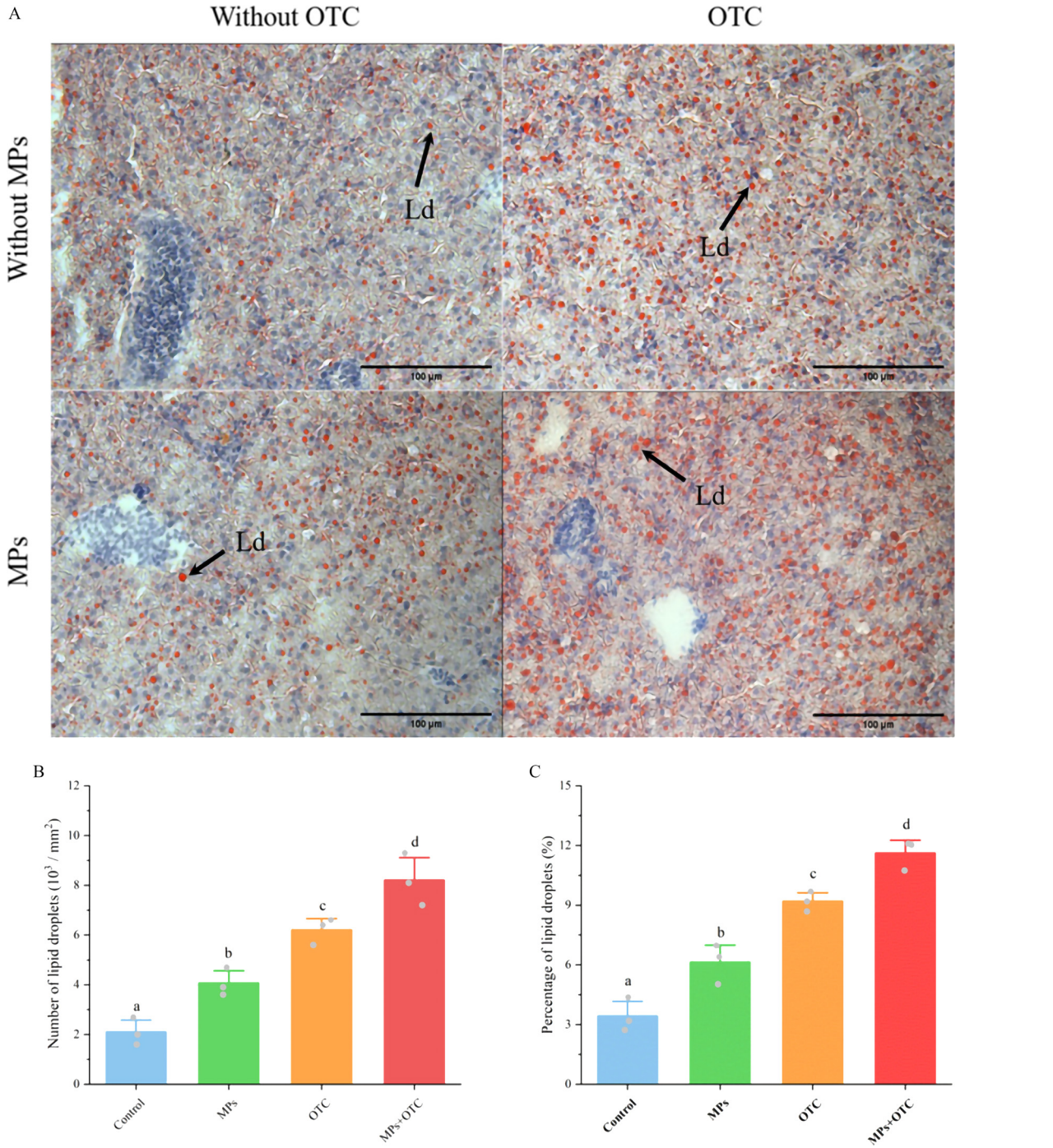


**Figure 1.** (A) Lipid droplet staining using Oil Red O ($n = 6$ and randomly selected images presented as representatives), (B) numbers of lipid droplets per millimeter squared ($n = 3$), and (C) quantified area of lipid droplets to that of the whole tissue observed ($n = 3$) in zebrafish livers after 28-d exposure to control, MPs, OTC, and MP-OTC, respectively. The black arrows in (A) indicate lipid droplets (Lds) (magnification at 200× and scale bar: 100 μm). Numbers of lipid droplets were counted manually and the percentages of lipid droplet area to that of the whole tissue observed were estimated with ImageJ in (B) and (C), respectively. The corresponding numeric data of (B) and (C) are provided in Table S4. Data (means ± SEs) with different superscripts above were significantly different at $p < 0.05$ (one-way analysis of variance and Tukey's post hoc tests). Note: MP-OTC, microplastics and oxytetracycline; MPs, microplastics; OTC, oxytetracycline; SE, standard error.

that of the control, respectively (Figure 6B). In this study, the highest F/B ratio was observed in zebrafish coexposed to MPs and OTC (Figure 6B).

### *Physiological Fitness of Zebrafish Intestines*

Compared with control, H&E staining of the intestine showed that zebrafish exposed to MPs, OTC, and MP-OTC harbored significantly fewer goblet cells (Figure 7A). Statistically, after 28-d treatment with MPs, OTC, and MP-OTC, the density of goblet cells was only ∼74.06%, 61.59%, and 40.72% of that of the control, respectively (Figure 7B; $F_{3,20} = 20.36$, $p < 0.05$). In addition, zebrafish from MPs-, OTC-, and MP-OTC–exposure groups exhibited MDA contents in their intestines that were ∼2.12, 1.22, and 3.41 times that of the control, respectively (Figure 8; $F_{3,20} = 118.15$, $p < 0.01$). Compared with those treated

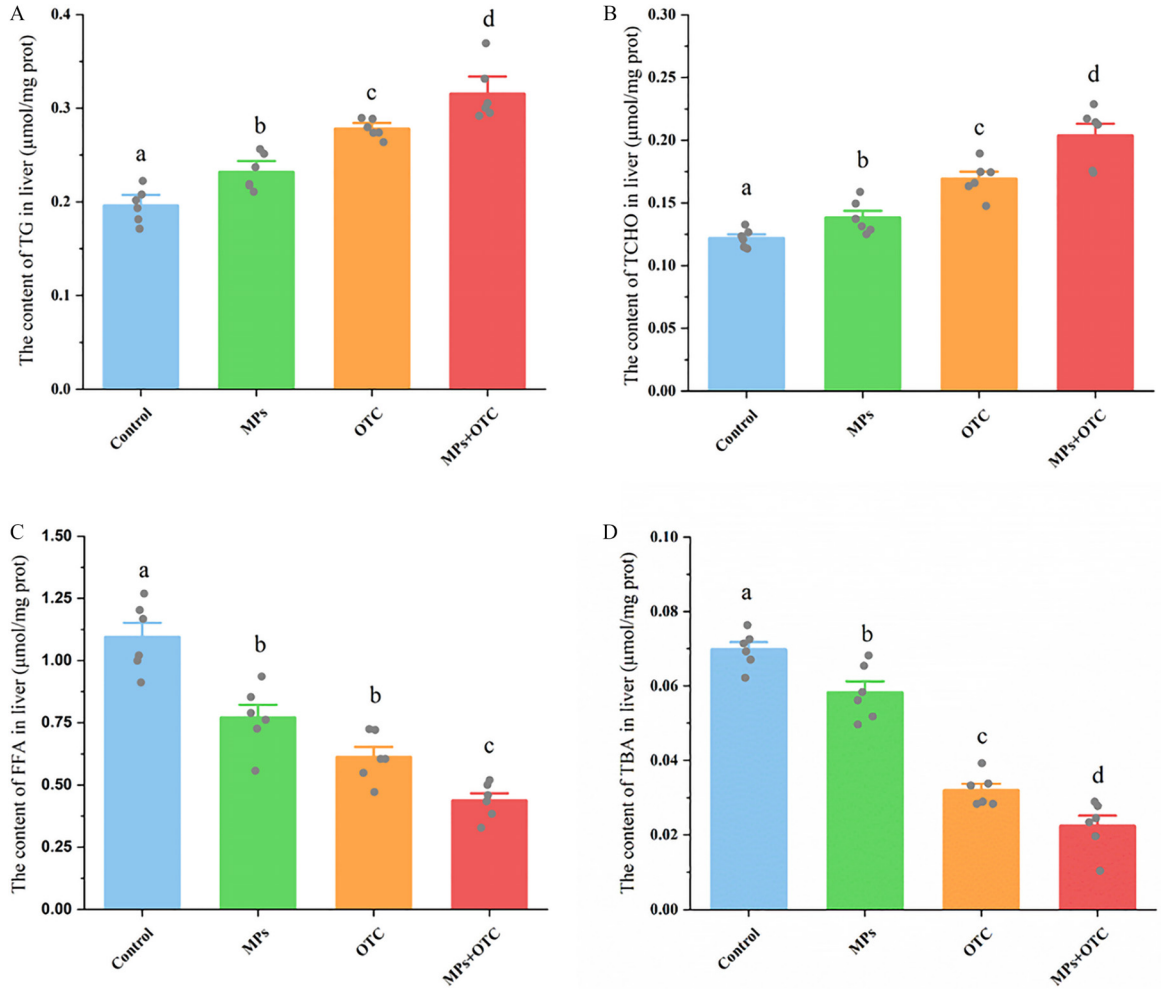


**Figure 2.** The contents of (A) triglycerides (TGs), (B) total cholesterol (TCHO), (C) free fatty acids (FFAs), and (D) total bile acids (TBAs) in zebrafish livers after 28-d exposure to control, MPs, OTC, and MP-OTC, respectively ($n = 6$ for each experimental group). All parameters were determined using corresponding commercial kits [BC0625, BC1985, and BC0595 (Solarbio) and E003-2-1 (Njjcbio), respectively] with a microplate reader (Multiskan GO; Thermo Scientific) and standardized with the protein content of the sample. The corresponding numeric data are provided in Table S5. Data (means ± SEs) with different superscripts above were significantly different at $p < 0.05$ (one-way analysis of variance and Tukey's post hoc tests). Note: MP-OTC, microplastics and oxytetracycline; MPs, microplastics; OTC, oxytetracycline; prot, protein; SE, standard error.

with MPs or OTC alone, zebrafish coexposed to MPs and OTC possessed significantly fewer goblet cells and a higher level of MDA content in their intestines (Figures 7 and 8).

### *Content of LPS in Serum and Expression of LBP in Liver*

The LPS levels in serum of MPs-, OTC-, and MP-OTC–treated zebrafish were ~1.15, 1.24, and 1.33 times that of the control, respectively (Figure 9A; $F_{3,20} = 35.62$, $p < 0.05$). After 28-d exposure of zebrafish to MPs, OTC, and MP-OTC, the expression levels of *LBP* in the livers were ~5.15-, 4.87-, and 10.64-fold that of the control, respectively (Figure 9B; $p < 0.05$). In addition, zebrafish coexposed to MPs and OTC yielded significantly higher levels of LPS in serum and *LBP* expression in liver than those treated with MPs or OTC alone (Figure 9).

### *Hepatic Lipid Catabolic Activity*

The activity of hepatic lipase in zebrafish exposed to MPs, OTC, and MP-OTC was ~6.67%, 9.71%, and 11.87% lower than that of control, respectively (Figure 10A; $F_{3,20} = 36.68$, $p < 0.05$). Although the MP-exposure group showed an *LIP* expression level that was similar to that of the control, significantly lower *LIP* expression was observed in the livers of zebrafish from the OTC- and the MP-OTC–exposure groups, ~74.98% and 42.48% of that of the control, respectively (Figure 10B; $F_{3,8} = 27.17$, $p < 0.05$). Compared with those treated with MPs or OTC alone, zebrafish coexposed to MPs and OTC revealed significantly lower lipase activity and *LIP* expression in their livers (Figure 10).

## Discussion

Regardless of the great threat posed by NAFLD prevalence on human health, the potential impacts of some emerging pollutants, such as MPs and OTC, to the development of NAFLD remains largely unknown. Data obtained in the present study demonstrate that zebrafish exposed to MPs and OTC at the levels equivalent to those reported by previous surveys[57–58] for 28 d exhibited a series of significant differences from control fish. This suggested the presence of NAFLD and was consistent with progression of the disease.

In addition to the most common NAFLD symptom of hepatic lipidosis [more and larger lipid droplets accumulated in hepatocytes (Figure 1), in conjunction with higher levels of TG and TCHO contents (Figure 2)], zebrafish exposed to MPs and OTC also displayed markedly higher expression levels of immune-related genes (*MyD88*, *TRAF6*, *NFκB*, and *TNF-α*), as well as TNF-α protein, in their livers (Figure 3). This supported the

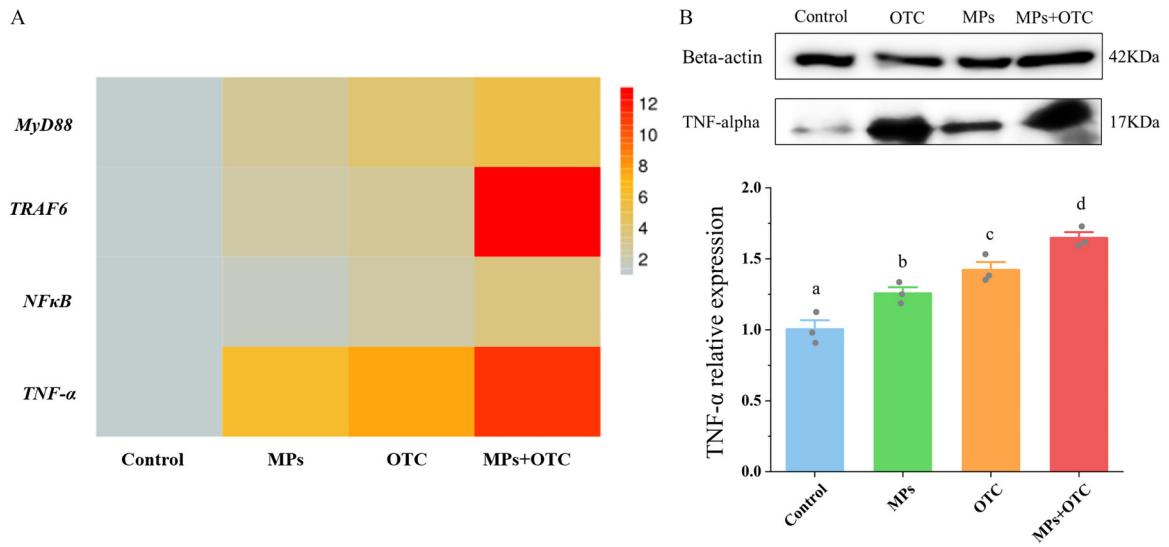


**Figure 3.** (A) Expression levels of inflammation-related genes and (B) western blot of TNF-α in zebrafish livers after 28-d exposure to control, MPs, OTC, and MP-OTC, respectively ($n = 3$ for each experimental group for both gene expression and western blot analyses). Gene expressions were determined by real-time PCR with a Bio-Rad real-time system (CFX96; Bio-Rad) and the relative TNF-α expression levels were quantified using ImageJ. The corresponding numeric data are provided in Table S6. Data (means ± SEs) with different superscripts above were significantly different at $p < 0.05$ (one-way analysis of variance and Tukey's post hoc tests). Note: MDA, malondialdehyde; MP-OTC, microplastics and oxytetracycline; MPs, microplastics; OTC, oxytetracycline; PCR, polymerase chain reaction; ROS, reactive oxygen species; SE, standard error; TNF-α, tumor necrosis factor-α.

presence of hepatic inflammation in these animals, a typical more severe symptom that was normally detected in the severe form of NAFLD, nonalcoholic steatohepatitis (NASH).[80–81] In addition, zebrafish exposed to MPs and OTC for 28 d revealed significantly higher levels of ROS and MDA (Figure 4), whereas lower activities of SOD and CAT (Figure 5) were found in their livers, suggesting the occurrence of oxidative injury (indicated by higher level of lipid peroxidation) probably due to an induction

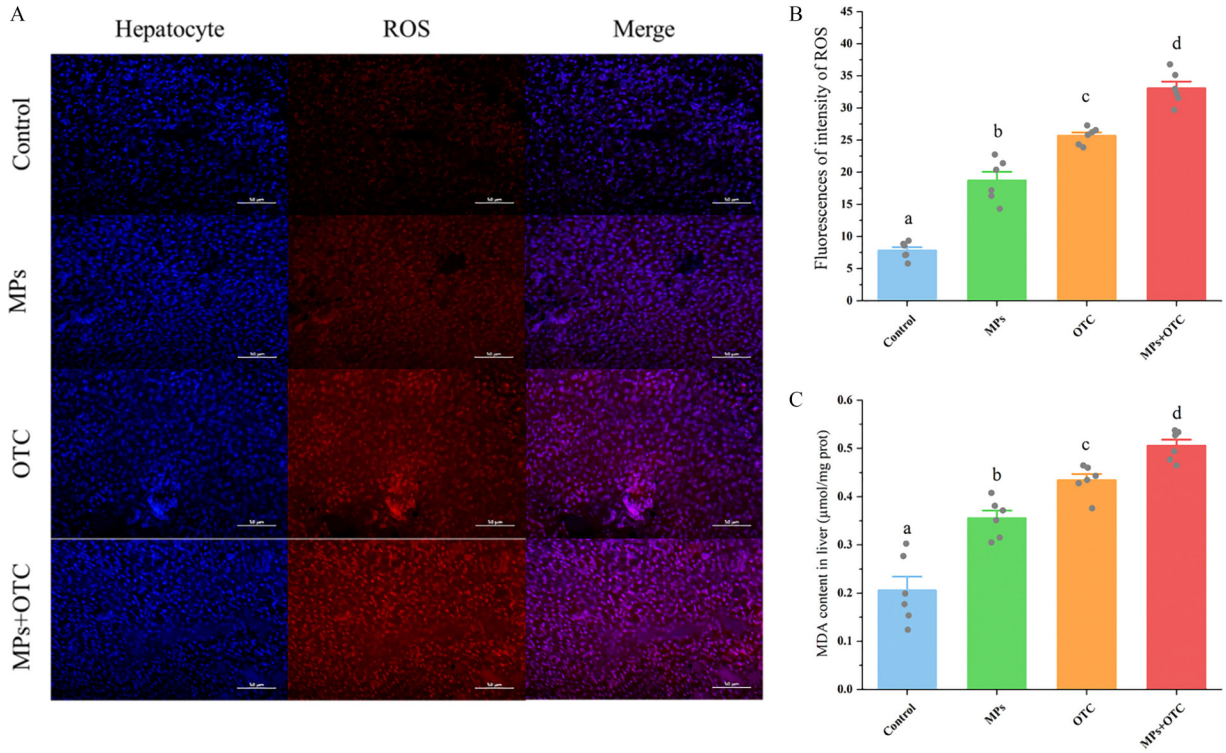


**Figure 4.** (A) ROS-specific fluorescent staining, (B) quantified ROS fluorescent intensities, and (C) MDA contents in zebrafish livers after 28-d exposure to control, MPs, OTC, and MP-OTC, respectively [$n = 6$ for each experimental group, and randomly selected images are presented as representatives for (A)]. The hepatocyte and ROS were stained in blue (DAPI) and red (DHE) in (A), respectively (magnification at 400× and scale bar: 50 μm). The ROS-specific fluorescence intensity was determined using ImageJ and the MDA content was measured with a commercial kit (BC0025; Solarbio) using a microplate reader (Multiskan GO; Thermo Scientific). The corresponding numeric data are provided in Table S7. Data (means ± SEs) with different superscripts above in (B) and (C) were significantly different between groups at $p < 0.05$ (one-way analysis of variance and Tukey's post hoc tests). Note: DAPI, 4′,6-diamidino-2-phenylindole; DHE, dihydroethidium; MDA, malondialdehyde; MP-OTC, microplastics and oxytetracycline; MPs, microplastics; OTC, oxytetracycline; prot, protein; ROS, reactive oxygen species; SE, standard error.

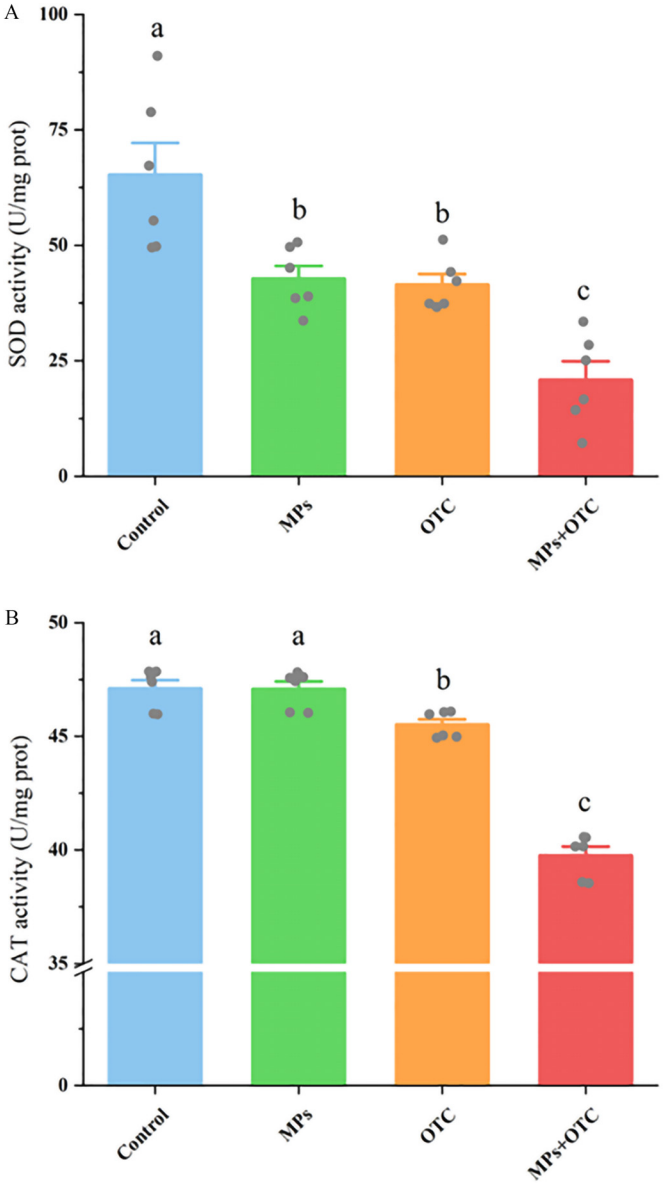


**Figure 5.** The activities of (A) SOD and (B) CAT in zebrafish livers after 28-d exposure to control, MPs, OTC, and MP-OTC, respectively ($n = 6$ for each experimental group). The enzymatic activities of SOD and CAT were measured with corresponding commercial kits (BC0175 and BC0205, respectively; Solarbio) using a microplate reader (Multiskan GO; Thermo Scientific). The corresponding numeric data are provided in Table S8. Data (means ± SEs) with different superscripts above were significantly different at $p < 0.05$ (one-way analysis of variance and Tukey's post hoc tests). Note: CAT, catalase; MP-OTC, microplastics and oxytetracycline; MPs, microplastics; OTC, oxytetracycline; prot, protein; SE, standard error; SOD, superoxide dismutase.

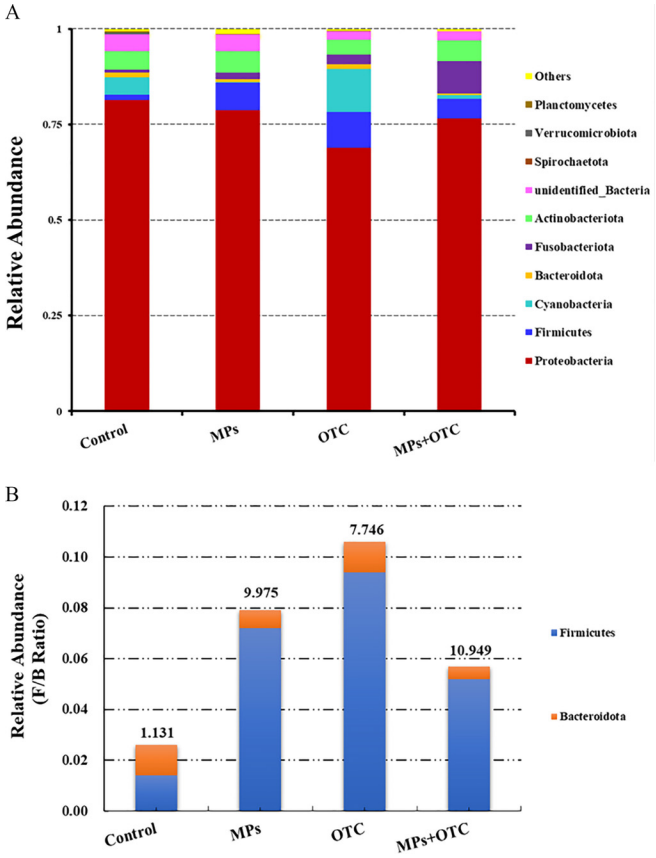


**Figure 6.** The (A) top 10 abundant microbial phyla and the (B) Firmicutes/Bacteroidetes ratios of the gut content microbiome of zebrafish after 28-d exposure to control, MPs, OTC, and MP-OTC, respectively ($n = 3$ for each experimental group). Microbiome of gut contents (under accession number of PRJNA890774 in NCBI database) were obtained by Illumina-based high-throughput sequencing (Novogene Co., Ltd.). Different microbial phyla are labeled with different colors and corresponding phyla names are listed on the right side in (A). Blue and orange colors in (B) indicate the relative abundance of Firmicutes and Bacteroidetes, respectively. The corresponding numeric data for (A) are provided in Table S9. The number above each data column in (B) indicates the Firmicutes/Bacteroidetes ratio for the corresponding experimental group. Note: F/B, Firmicutes/Bacteroidetes (ratio); MP-OTC, microplastics and oxytetracycline; MPs, microplastics; NCBI, National Center for Biotechnology Information; OTC, oxytetracycline.

of *in vivo* ROS and a disruption of antioxidant enzymes. Given that high degrees of lipidosis, extensive inflammation, and pathological lesions often progress to severe liver diseases, such as hepatocyte necrosis,[82] hepatocyte fibrosis,[83] and liver cirrhosis,[84] our results give an indication where exposure to environmental MPs and OTC could pose a considerable threat to liver health.

Based on the data obtained in this study, we hypothesize that the gut–liver axis might be the target of MPs and OTC in zebrafish with NAFLD. First, microbiome analysis of gut contents showed that zebrafish from the MPs-, OTC-, and MP-OTC–exposure groups yielded a smaller relative abundance of Proteobacteria but higher F/B ratios compared with that of the control fish (Figure 6), which the authors postulate to be a sign of gut microbiota dysbiosis. According to previous studies,[74–75] a high F/B ratio might be an important indicator of obesity, a common complication of NAFLD, thus the higher F/B ratios observed in zebrafish after 28-d exposure to MPs and OTC may suggest a higher risk of obesity and NAFLD. In addition, it has been suggested that change in microbial composition of the gut may increase the release of intestinal endotoxins, such as LPS.[85–86] Based on the relationship between intestinal microbial composition and LPS release reported in zebrafish,[87] we reason that zebrafish exposed to MPs and OTC might have higher levels of LPS in their intestines due to the reduced abundance of the dominant microbial Proteobacteria in their gut contents.

In accordance with previous studies,[76–77] our data showed that zebrafish exposed to MPs and OTC for 28 d exhibited significantly higher MDA contents and fewer goblet cells in their intestines than the control fish (Figures 7 and 8). On one hand, the higher MDA contents observed suggested the occurrence of intestinal oxidative injury in MPs- and OTC-treated zebrafish, which is believed by the authors to be the potential cause for the fewer goblet cells detected. On the other hand, given that intestinal mucus (the mucosal barrier on the intestinal surface that

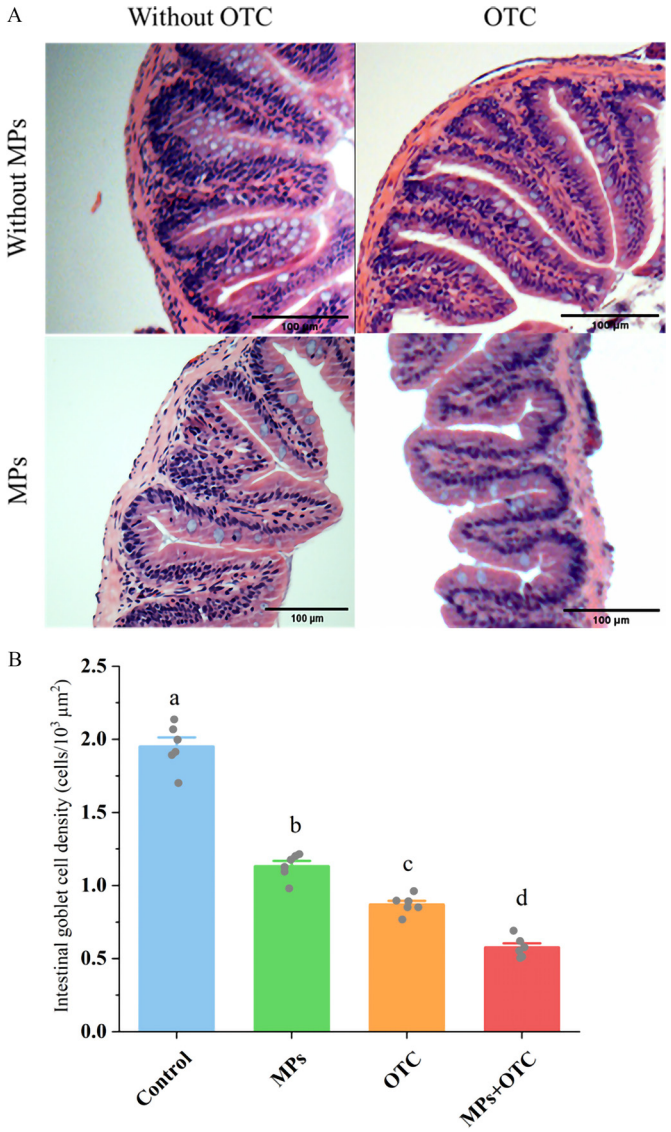


**Figure 7.** (A) Histological images of intestines and (B) quantified intestinal goblet cell densities in zebrafish exposed to control, MPs, OTC, and MP-OTC, respectively [$n = 6$ for both analysis for each experimental group, and randomly selected images are presented as representatives for (A)]. The images of intestines presented in (A) were stained with H&E. The magnification and scale bar were 200× and 100 μm for (A), respectively. Goblet cells are indicated by black arrows in (A). The corresponding numeric data for (B) are provided in Table S10. Data (means ± SEs) with different superscripts above were significantly different at $p < 0.05$ (one-way analysis of variance and Tukey's post hoc tests). Note: H&E, hematoxylin and eosin; MP-OTC, microplastics and oxytetracycline; MPs, microplastics; OTC, oxytetracycline; SE, standard error.

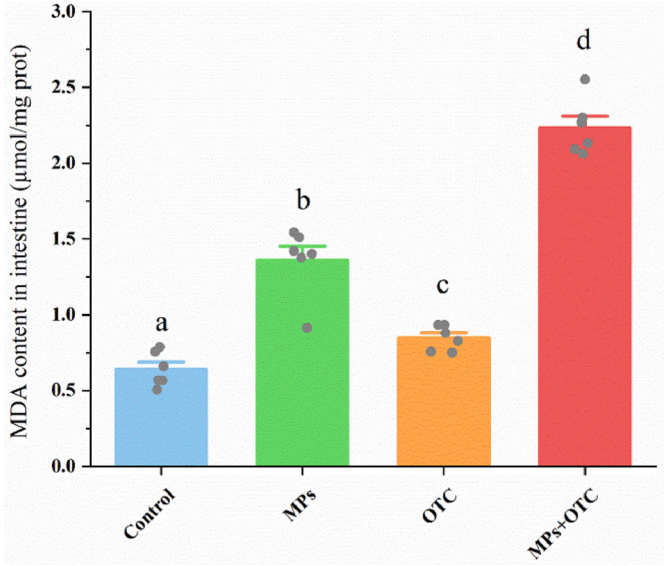


**Figure 8.** MDA contents in the intestines of zebrafish after 28-d exposure to control, MPs, OTC, and MP-OTC, respectively ($n = 6$ for each experimental group). The MDA content was measured with a commercial kit (BC0025; Solarbio) using a microplate reader (Multiskan GO; Thermo Scientific) and standardized with the protein content of the sample. The corresponding numeric data are provided in Table S11. Data (means ± SEs) with different superscripts above were significantly different at $p < 0.05$ (one-way analysis of variance and Tukey's post hoc tests). Note: MDA, malondialdehyde; MP-OTC, microplastics and oxytetracycline; MPs, microplastics; OTC, oxytetracycline; prot, protein; SE, standard error.

prevents harmful substances from entering the circulatory system) was primarily secreted by goblet cells,[88–89] we hypothesize that MPs- and OTC-treated zebrafish with fewer goblet cells in their intestines may have a disrupted intestinal mucosal barrier and thus higher intestinal permeability to harmful substances, such as endotoxins.

In this study, significantly higher levels of LPS were detected in the serum of zebrafish after 28-d exposure (Figure 9A). Meanwhile, MPs- and OTC-treated zebrafish exhibited higher levels of *LBP* compared with the control (Figure 9B). One interpretation of this finding might be the activation of the LBP by high levels of LPS. According to the literature, once activated by the potent endotoxin LPS, a series of immune responses will be triggered,[78,90] offering a probable explanation for the inflammatory symptoms detected. Specifically, we found higher levels of *MyD88*, *NFκB*, *TRAF6*, and *TNF-α*, as well as TNF-α in the livers of zebrafish exposed to MPs and OTC, suggesting that LPS binding to its receptor, LBP, may activate *MyD88*, triggering the downstream *NFκB*-signaling pathway and the release of pro-inflammatory TNF-α.

According to previous studies,[63,91] both inflammation and oxidative injury of the liver induced by exposure of zebrafish to MPs and OTC could lead to hepatic lipid metabolism disorders, which may give rise to hepatic lipidosis. For instance, it has been demonstrated that lipid peroxidation caused by oxidative stress could damage hepatocytes and inhibit normal hepatic lipid metabolism in zebrafish.[92] In addition, it has been shown that zebrafish lipase was sensitive to oxidative stress and inflammation.[92–93] In accordance with these previous studies, our data illustrated that zebrafish exposed to MPs and OTC for 28 d produced significantly lower activity of hepatic lipase and *LIP* expression than that of the control fish (Figure 10). In addition, MPs- and OTC-treated zebrafish harbored markedly less FFA and TBA (catabolites for TG and TCHO, respectively) in their livers (Figure 2C,D). We believe that the observation of low levels of FFAs and TBA under high levels of TG and TCHO in the livers of MPs- and OTC-treated zebrafish indicates a significant reduction in lipid catabolism, which may partially account for the excessive accumulation of lipids in the liver. Furthermore, it has been suggested that the pro-inflammatory factor TNF-α could interfere with insulin signaling and lead to insulin resistance,[94] which might be not only the primary cause of diabetes but also closely related to obesity progression[95–96] and NAFLD.[97–98] Thus, in addition to disrupting hepatic lipid metabolism, we believe that interfering with insulin signaling could be another route for the incidence and progression of NAFLD observed in MPs- and OTC-treated zebrafish.

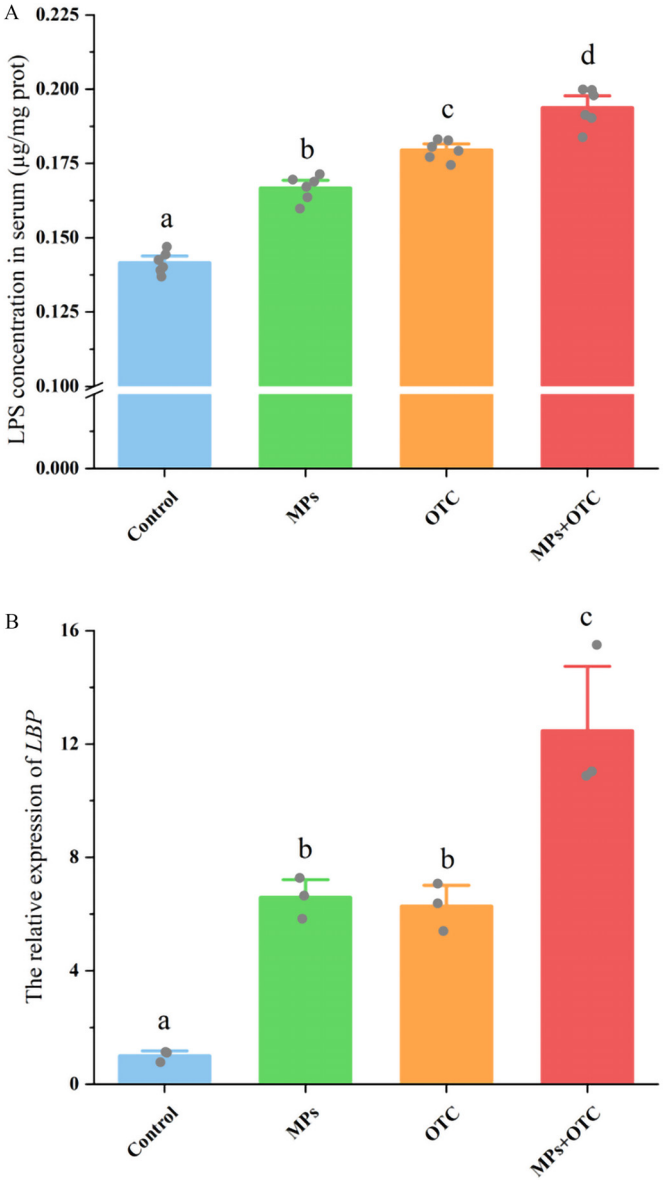


**Figure 9.** (A) LPS contents in serum ($n=6$ for each experimental group) and (B) expression levels of *LBP* in the livers ($n=3$ for each experimental group of zebrafish after 28-d exposure to control, MPs, OTC, and MP-OTC, respectively). The LPS content in the sample was measured with the commercial LPS ELISA kit (JL13861; Jonln Biotechnology) using a microplate reader (Multiskan GO; Thermo Scientific), and *LBP* expression was determined by real-time PCR with a Bio-Rad real-time system (CFX96; Bio-Rad). The corresponding numeric data are provided in Table S12. Data (means ± SEs) with different superscripts above were significantly different at $p<0.05$ (one-way analysis of variance and Tukey's post hoc tests). Note: ELISA, enzyme-linked immunosorbent assay; *LBP*, gene encoding lipopolysaccharide binding receptor; LPS, lipopolysaccharide; MP-OTC, microplastics and oxytetracycline; MPs, microplastics; OTC, oxytetracycline; PCR, polymerase chain reaction; prot, protein; SE, standard error.

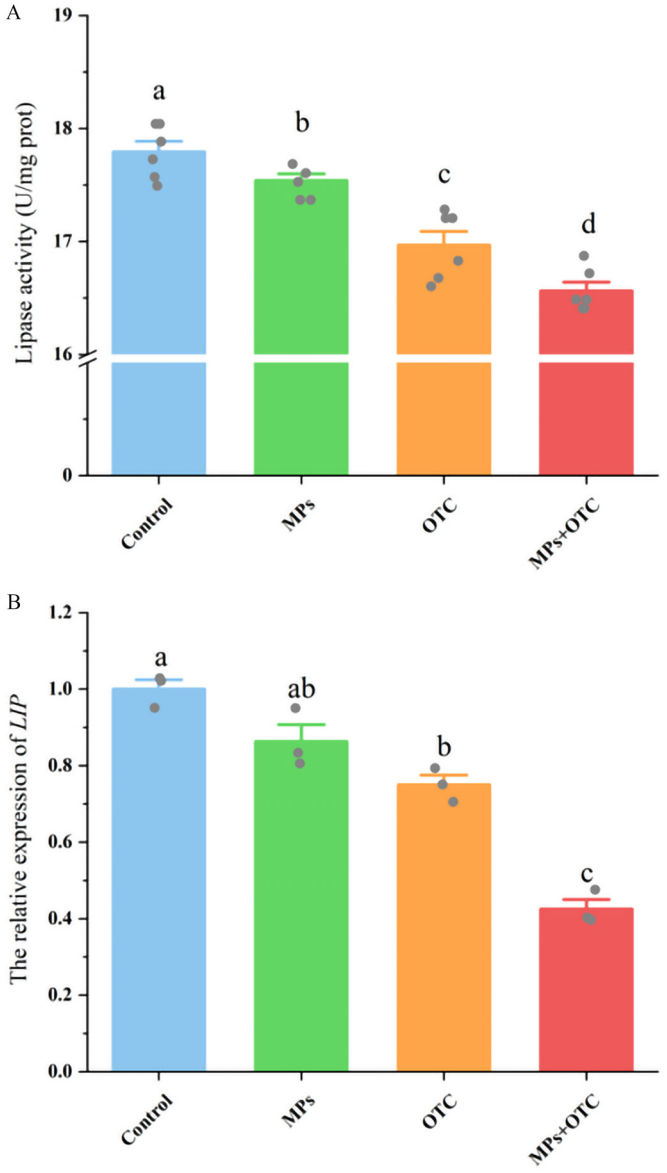


**Figure 10.** (A) Activities of lipase ($n=6$ for each experimental group) and (B) expressions of *LIP* ($n=3$ for each experimental group) in zebrafish livers after 28-d exposure to control, MPs, OTC, and MP-OTC, respectively. The activity of lipase was determined with the commercial lipase activity kit (BC2345; Solarbio) using a microplate reader (Multiskan GO; Thermo Scientific) and *LIP* expression was determined by real-time PCR with a Bio-Rad real-time system (CFX96; Bio-Rad). The corresponding numeric data are provided in Table S13. Data (means ± SEs) with different superscripts above were significantly different at $p<0.05$ (one-way analysis of variance and Tukey's post hoc tests). Note: *LIP*, gene encoding lipase; MP-OTC, microplastics and oxytetracycline; MPs, microplastics; OTC, oxytetracycline; PCR, polymerase chain reaction; prot, protein; SE, standard error.

Complementing previous studies carried out in other species (i.e., the thick-shell mussel[99] and the blood clam[71]), our study found coexposure of zebrafish to MPs and OTC generally exerted more severe effects on the parameters investigated compared with single treatments. On one hand, this may be due to the summation of adverse impacts on shared common targets (i.e., almost all the physiological parameters investigated in this study) of MPs and OTC. On the other hand, according to the intestinal OTC accumulation (Figure S2) and the FT-IR results (Figure S3) of the present study and those reported previously,[32,36] MPs could also absorb OTC residues from the environment (the aqueous environment in the present study). Therefore, we hypothesized that MPs may condense environmental OTC and act as vectors to facilitate the internalization of OTC, which could be another explanation for the more severe impacts detected.

Due to the frequent detection of MPs and OTC in food materials,[100–101] sauces,[19] and drinking water,[28,58] ingestion through contaminated food and drinking water has been suggested to be the primary exposure route in humans.[102–103] For example, it has been demonstrated that the average MPs in five frequently consumed

fruits and vegetables (apples, pears, broccoli, lettuce, and carrots) in Catania, Italy, reached as high as 132,740 particles/g.[104] In addition, based on the survey conducted in Catania, Italy,[28] the estimated daily intakes of MPs through drinking bottled water were estimated to be $\sim 1.53 \times 10^6$ particles/kg-body weight (BW) per day (40.1 mg/kg-BW per day) and $3.35 \times 10^6$ particles/kg-BW per day (87.8 mg/kg-BW per day) for adults and children, respectively. Furthermore, given the exposure risk caused by consuming formula prepared in infant feeding bottles, the daily intake of MPs by infants was estimated to be $\sim 1.62 \times 10^7$ particles/day based on data collected from 48 regions globally.[105] Similarly, the estimated daily intakes of OTC merely through consuming contaminated seafood was estimated to be $\sim 0.141$–$0.447$ μg/d per capita based on the survey results ($\sim 2.7$–$8.6$ μg/kg OTC) of seafood in the U.S. market[48] and the seafood consumption per capita (52.05 g/d) of the Food and Agriculture Organization of the United Nations.[106]

Although both MPs and OTC potentially pose a great threat to human health, the realistic overall exposure concentrations of these two pollutants remain unclear. Therefore, it is hard to directly extrapolate the results obtained in this study to humans (the zebrafish were exposed to the environmental realistic concentrations of MPs and OTC for fish species). However, given the high genome sequence homologies between human and zebrafish,[107] our results contribute significant implications for the environmental induction of human NAFLD. Considering the long-term amount of MPs and OTC that can accumulate in our body via daily ingestion of contaminated food and water, the potential NAFLD risk of these pollutants should not be overlooked.

## Acknowledgments

W.S.Z., W.S., and G.X.L. contributed to experimental design, statistical analysis and manuscript preparation. W.S.Z., W.S., and X.Y.D. carried out the experiments; Y.H., Y.T., S.H.R., K.J.J., T.C.K., L.H., W.X.Z., Y.H.Y., D.D.T., L.B.C., W.Z.C., and Y.Y.Y. contributed to experiment preparation and data analysis. G.X.L. contributed to substantive discussion of the results and revision of the manuscript.

This work was funded by the National Key R&D Program of China (no. 2018YFD0900601), the National Natural Science Foundation of China (no. 32172944), the Natural Science Foundation of Zhejiang Province (LQ21C190003), and the Open Fund of Zhejiang Key Laboratory of Exploration and Preservation of Costal Bio-resources (J2021001).

## References

1. Pais R, Maurel T. 2021. Natural history of NAFLD. J Clin Med 10(6):1161, PMID: 33802047, https://doi.org/10.3390/jcm10061161.
2. Younossi ZM, Koenig AB, Abdelatif D, Fazel Y, Henry L, Wymer M. 2016. Global epidemiology of nonalcoholic fatty liver disease—meta-analytic assessment of prevalence, incidence, and outcomes. Hepatology 64(1):73–84, PMID: 26707365, https://doi.org/10.1002/hep.28431.
3. Younossi Z, Tacke F, Arrese M, Chander Sharma B, Mostafa I, Bugianesi E, et al. 2019. Global perspectives on nonalcoholic fatty liver disease and nonalcoholic steatohepatitis. Hepatology 69(6):2672–2682, PMID: 30179269, https://doi.org/10.1002/hep.30251.
4. Fu JF, Shi HB, Liu LR, Jiang P, Liang L, Wang CL, et al. 2011. Non-alcoholic fatty liver disease: an early mediator predicting metabolic syndrome in obese children? World J Gastroenterol 17(6):735–742, PMID: 21390143, https://doi.org/10.3748/wjg.v17.i6.735.
5. Fan JG. 2013. Epidemiology of alcoholic and nonalcoholic fatty liver disease in China. J Gastroenterol Hepatol 28(suppl 1):11–17, PMID: 23855290, https://doi.org/10.1111/jgh.12036.
6. Estes C, Razavi H, Loomba R, Younossi Z, Sanyal AJ. 2018. Modeling the epidemic of nonalcoholic fatty liver disease demonstrates an exponential increase in burden of disease. Hepatology 67(1):123–133, PMID: 28802062, https://doi.org/10.1002/hep.29466.
7. O'Neill S, O'Driscoll L. 2015. Metabolic syndrome: a closer look at the growing epidemic and its associated pathologies. Obes Rev 16(1):1–12, PMID: 25407540, https://doi.org/10.1111/obr.12229.
8. Arciello M, Gori M, Maggio R, Barbaro B, Tarocchi M, Galli A, et al. 2013. Environmental pollution: a tangible risk for NAFLD pathogenesis. Int J Mol Sci 14(11):22052–22066, PMID: 24213605, https://doi.org/10.3390/ijms141122052.
9. Rajak S, Raza S, Tewari A, Sinha RA. 2022. Environmental toxicants and NAFLD: a neglected yet significant relationship. Dig Dis Sci 67(8):3497–3507, PMID: 34383198, https://doi.org/10.1007/s10620-021-07203-y.
10. Zheng Z, Xu X, Zhang X, Wang A, Zhang C, Hüttemann M, et al. 2013. Exposure to ambient particulate matter induces a NASH-like phenotype and impairs hepatic glucose metabolism in an animal model. J Hepatol 58(1):148–154, PMID: 22902548, https://doi.org/10.1016/j.jhep.2012.08.009.
11. Yang D, Zhang X, Yue L, Hu H, Wei X, Guo Q, et al. 2021. Thiamethoxam induces nonalcoholic fatty liver disease in mice via methionine metabolism disturb via nicotinamide N-methyltransferase overexpression. Chemosphere 273:129727, PMID: 33524747, https://doi.org/10.1016/j.chemosphere.2021.129727.
12. Verstraete SG, Wojcicki JM, Perito ER, Rosenthal P. 2018. Bisphenol A increases risk for presumed non-alcoholic fatty liver disease in Hispanic adolescents in NHANES 2003–2010. Environ Health 17(1):12, PMID: 29391015, https://doi.org/10.1186/s12940-018-0356-3.
13. Angrish MM, Dominici CY, Zacharewski TR. 2013. TCDD-elicited effects on liver, serum, and adipose lipid composition in C57BL/6 mice. Toxicol Sci 131(1):108–115, PMID: 22977169, https://doi.org/10.1093/toxsci/kfs277.
14. Geyer R, Jambeck JR, Law KL. 2017. Production, use, and fate of all plastics ever made. Sci Adv 3(7):e1700782, PMID: 28776036, https://doi.org/10.1126/sciadv.1700782.
15. Okoffo ED, Donner E, McGrath SP, Tscharke BJ, O'Brien JW, O'Brien S, et al. 2021. Plastics in biosolids from 1950 to 2016: a function of global plastic production and consumption. Water Res 201:117367, PMID: 34182349, https://doi.org/10.1016/j.watres.2021.117367.
16. PlasticsEurope. 2021. Plastics—the facts 2021: an analysis of European plastics production, demand and waste data. https://plasticseurope.org/knowledge-hub/plastics-the-facts-2021/ [accessed 5 March 2022].
17. Geyer R. 2020. Chapter 2—production, use, and fate of synthetic polymers. In: *Plastic Waste and Recycling: Environmental Impact, Societal Issues, Prevention, and Solutions*. Letcher T, ed. New York, NY: Academic Press, 13–32.
18. Danso D, Chow J, Streit WR. 2019. Plastics: environmental and biotechnological perspectives on microbial degradation. Appl Environ Microbiol 85(19):e01095-19, PMID: 31324632, https://doi.org/10.1128/AEM.01095-19.
19. Peixoto D, Pinheiro C, Amorim J, Oliva-Teles L, Guilhermino L, Vieira MN. 2019. Microplastic pollution in commercial salt for human consumption: a review. Estuar Coast Shelf Sci 219:161–168, https://doi.org/10.1016/j.ecss.2019.02.018.
20. Fan P, Yu H, Xi B, Tan W. 2022. A review on the occurrence and influence of biodegradable microplastics in soil ecosystems: are biodegradable plastics substitute or threat? Environ Int 163:107244, PMID: 35436719, https://doi.org/10.1016/j.envint.2022.107244.
21. Arp HPH, Kühnel D, Rummel C, MacLeod M, Potthoff A, Reichelt S, et al. 2021. Weathering plastics as a planetary boundary threat: exposure, fate, and hazards. Environ Sci Technol 55(11):7246–7255, PMID: 33973471, https://doi.org/10.1021/acs.est.1c01512.
22. Summers S, Henry T, Gutierrez T. 2018. Agglomeration of nano- and microplastic particles in seawater by autochthonous and de novo-produced sources of exopolymeric substances. Mar Pollut Bull 130:258–267, PMID: 29866555, https://doi.org/10.1016/j.marpolbul.2018.03.039.
23. Gouin T, Roche N, Lohmann R, Hodges G. 2011. A thermodynamic approach for assessing the environmental exposure of chemicals absorbed to microplastic. Environ Sci Technol 45(4):1466–1472, PMID: 21268630, https://doi.org/10.1021/es1032025.
24. Thompson RC, Olsen Y, Mitchell RP, Davis A, Rowland SJ, John AWG, et al. 2004. Lost at sea: where is all the plastic? Science 304(5672):838, PMID: 15131299, https://doi.org/10.1126/science.1094559.
25. Domenech J, Marcos R. 2021. Pathways of human exposure to microplastics, and estimation of the total burden. Curr Opin Food Sci 39:144–151, https://doi.org/10.1016/j.cofs.2021.01.004.
26. De Falco F, Gullo MP, Gentile G, Di Pace E, Cocca M, Gelabert L, et al. 2018. Evaluation of microplastic release caused by textile washing processes of synthetic fabrics. Environ Pollut 236:916–925, PMID: 29107418, https://doi.org/10.1016/j.envpol.2017.10.057.
27. Liu K, Wang X, Wei N, Song Z, Li D. 2019. Accurate quantification and transport estimation of suspended atmospheric microplastics in megacities: implications for human health. Environ Int 132:105127, PMID: 31487610, https://doi.org/10.1016/j.envint.2019.105127.
28. Zuccarello P, Ferrante M, Cristaldi A, Copat C, Grasso A, Sangregorio D, et al. 2019. Exposure to microplastics (<10 μm) associated to plastic bottles mineral water consumption: the first quantitative study. Water Res 157:365–371, PMID: 30974285, https://doi.org/10.1016/j.watres.2019.03.091.
29. Leslie HA, van Velzen MJM, Brandsma SH, Vethaak AD, Garcia-Vallejo JJ, Lamoree MH. 2022. Discovery and quantification of plastic particle pollution

in human blood. Environ Int 163:107199, PMID: 35367073, https://doi.org/10.1016/j.envint.2022.107199.
30. Ragusa A, Svelato A, Santacroce C, Catalano P, Notarstefano V, Carnevali O, et al. 2021. Plasticenta: first evidence of microplastics in human placenta. Environ Int 146:106274, PMID: 33395930, https://doi.org/10.1016/j.envint.2020.106274.
31. Xu B, Liu F, Brookes PC, Xu J. 2018. The sorption kinetics and isotherms of sulfamethoxazole with polyethylene microplastics. Mar Pollut Bull 131(pt A):191–196, PMID: 29886936, https://doi.org/10.1016/j.marpolbul.2018.04.027.
32. Zhang H, Wang J, Zhou B, Zhou Y, Dai Z, Zhou Q, et al. 2018. Enhanced adsorption of oxytetracycline to weathered microplastic polystyrene: kinetics, isotherms and influencing factors. Environ Pollut 243(pt B):1550–1557, PMID: 30296753, https://doi.org/10.1016/j.envpol.2018.09.122.
33. Yu F, Li Y, Huang G, Yang C, Chen C, Zhou T, et al. 2020. Adsorption behavior of the antibiotic levofloxacin on microplastics in the presence of different heavy metals in an aqueous solution. Chemosphere 260:127650, PMID: 32693263, https://doi.org/10.1016/j.chemosphere.2020.127650.
34. Zhou W, Han Y, Tang Y, Shi W, Du X, Sun S, et al. 2020. Microplastics aggravate the bioaccumulation of two waterborne veterinary antibiotics in an edible bivalve species: potential mechanisms and implications for human health. Environ Sci Technol 54(13):8115–8122, PMID: 32531169, https://doi.org/10.1021/acs.est.0c01575.
35. Guilhermino L, Vieira LR, Ribeiro D, Tavares AS, Cardoso V, Alves A, et al. 2018. Uptake and effects of the antimicrobial florfenicol, microplastics and their mixtures on freshwater exotic invasive bivalve *Corbicula fluminea*. Sci Total Environ 622–623:1131–1142, PMID: 29890582, https://doi.org/10.1016/j.scitotenv.2017.12.020.
36. Li J, Zhang K, Zhang H. 2018. Adsorption of antibiotics on microplastics. Environ Pollut 237:460–467, PMID: 29510365, https://doi.org/10.1016/j.envpol.2018.02.050.
37. Verdú I, González-Pleiter M, Leganés F, Rosal R, Fernández-Piñas F. 2021. Microplastics can act as vector of the biocide triclosan exerting damage to freshwater microalgae. Chemosphere 266:129193, PMID: 33310522, https://doi.org/10.1016/j.chemosphere.2020.129193.
38. Klein EY, Van Boeckel TP, Martinez EM, Pant S, Gandra S, Levin SA, et al. 2018. Global increase and geographic convergence in antibiotic consumption between 2000 and 2015. Proc Natl Acad Sci USA 115(15):E3463–E3470, PMID: 29581252, https://doi.org/10.1073/pnas.1717295115.
39. Robles-Jimenez LE, Aranda-Aguirre E, Castelan-Ortega OA, Shettino-Bermudez BS, Ortiz-Salinas R, Miranda M, et al. 2021. Worldwide traceability of antibiotic residues from livestock in wastewater and soil: a systematic review. Animals (Basel) 12(1):60, PMID: 35011166, https://doi.org/10.3390/ani12010060.
40. Booth A, Aga DS, Wester AL. 2020. Retrospective analysis of the global antibiotic residues that exceed the predicted no effect concentration for antimicrobial resistance in various environmental matrices. Environ Int 141:105796, PMID: 32422499, https://doi.org/10.1016/j.envint.2020.105796.
41. Alcock RE, Sweetman A, Jones KC. 1999. Assessment of organic contaminant fate in waste water treatment plants. I: selected compounds and physicochemical properties. Chemosphere 38(10):2247–2262, PMID: 10101865, https://doi.org/10.1016/S0045-6535(98)00444-5.
42. Li YW, Wu XL, Mo CH, Tai YP, Huang XP, Xiang L. 2011. Investigation of sulfonamide, tetracycline, and quinolone antibiotics in vegetable farmland soil in the Pearl River Delta area, southern China. J Agric Food Chem 59(13):7268–7276, PMID: 21623636, https://doi.org/10.1021/jf1047578.
43. Chen L, Lang H, Liu F, Jin S, Yan T. 2018. Presence of antibiotics in shallow ground water in the northern and southwestern regions of China. Ground Water 56(3):451–457, PMID: 28940442, https://doi.org/10.1111/gwat.12596.
44. Jiang Y, Li M, Guo C, An D, Xu J, Zhang Y, et al. 2014. Distribution and ecological risk of antibiotics in a typical effluent-receiving river (Wangyang River) in north China. Chemosphere 112:267–274, PMID: 25048915, https://doi.org/10.1016/j.chemosphere.2014.04.075.
45. Hebbal MA, Latha C, Menon KV, Deepa J. 2020. Occurrence of oxytetracycline residues in milk samples from Palakkad, Kerala, India. Vet World 13(6):1056–1064, PMID: 32801555, https://doi.org/10.14202/vetworld.2020.1056-1064.
46. Olatoye O, Kayode ST. 2012. Oxytetracycline residues in retail chicken eggs in Ibadan, Nigeria. Food Addit Contam Part B Surveill 5(4):255–259, PMID: 24786405, https://doi.org/10.1080/19393210.2012.702791.
47. Gunes ME, Gunes N, Cibik R. 2009. Oxytetracycline and sulphonamide residues analysis of honey samples from Southern Marmara region in Turkey. Bulg J Agric Sci 15:163–167.
48. Done HY, Halden RU. 2015. Reconnaissance of 47 antibiotics and associated microbial risks in seafood sold in the United States. J Hazard Mater 282:10–17, PMID: 25449970, https://doi.org/10.1016/j.jhazmat.2014.08.075.
49. Ribeiro CFA, Silveira GGOS, Cândido ES, Cardoso MH, Espínola Carvalho CM, Franco OL. 2020. Effects of antibiotic treatment on gut microbiota and how to overcome its negative impacts on human health. ACS Infect Dis 6(10):2544–2559, PMID: 32786282, https://doi.org/10.1021/acsinfecdis.0c00036.
50. Compare D, Coccoli P, Rocco A, Nardone OM, De Maria S, Cartenì M, et al. 2012. Gut–liver axis: the impact of gut microbiota on non alcoholic fatty liver disease. Nutr Metab Cardiovasc Dis 22(6):471–476, PMID: 22546554, https://doi.org/10.1016/j.numecd.2012.02.007.
51. Ohtani N, Kawada N. 2019. Role of the gut–liver axis in liver inflammation, fibrosis, and cancer: a special focus on the gut microbiota relationship. Hepatol Commun 3(4):456–470, PMID: 30976737, https://doi.org/10.1002/hep4.1331.
52. Dong CD, Chen CW, Chen YC, Chen HH, Lee JS, Lin CH. 2020. Polystyrene microplastic particles: in vitro pulmonary toxicity assessment. J Hazard Mater 385:121575, PMID: 31727530, https://doi.org/10.1016/j.jhazmat.2019.121575.
53. Jiang J, Chen L, Wu S, Lv L, Liu X, Wang Q, et al. 2020. Effects of difenoconazole on hepatotoxicity, lipid metabolism and gut microbiota in zebrafish (*Danio rerio*). Environ Pollut 265(pt A):114844, PMID: 32480235, https://doi.org/10.1016/j.envpol.2020.114844.
54. Kirpich IA, Marsano LS, McClain CJ. 2015. Gut–liver axis, nutrition, and non-alcoholic fatty liver disease. Clin Biochem 48(13–14):923–930, PMID: 26151226, https://doi.org/10.1016/j.clinbiochem.2015.06.023.
55. Goessling W, Sadler KC. 2015. Zebrafish: an important tool for liver disease research. Gastroenterology 149(6):1361–1377, PMID: 26319012, https://doi.org/10.1053/j.gastro.2015.08.034.
56. Pham DH, Zhang C, Yin C. 2017. Using zebrafish to model liver diseases—where do we stand? Curr Pathobiol Rep 5(2):207–221, PMID: 29098121, https://doi.org/10.1007/s40139-017-0141-y.
57. Liong RMY, Hadibarata T, Yuniarto A, Tang KHD, Khamidun MH. 2021. Microplastic occurrence in the water and sediment of Miri River Estuary, Borneo Island. Water Air Soil Pollut 232(8):342, https://doi.org/10.1007/s11270-021-05297-8.
58. Qin Y, Wen Q, Ma Y, Yang C, Liu Z. 2018. Antibiotics pollution in Gonghu Bay in the period of water diversion from Yangtze River to Taihu Lake. Environ Earth Sci 77(11):419, https://doi.org/10.1007/s12665-018-7558-4.
59. Jiang L, Hu X, Yin D, Zhang H, Yu Z. 2011. Occurrence, distribution and seasonal variation of antibiotics in the Huangpu River, Shanghai, China. Chemosphere 82(6):822–828, PMID: 21131021, https://doi.org/10.1016/j.chemosphere.2010.11.028.
60. Song YK, Hong SH, Jang M, Han GM, Rani M, Lee J, et al. 2015. A comparison of microscopic and spectroscopic identification methods for analysis of microplastics in environmental samples. Mar Pollut Bull 93(1–2):202–209, PMID: 25682567, https://doi.org/10.1016/j.marpolbul.2015.01.015.
61. Chen Y, Li J, Wang F, Yang H, Liu L. 2021. Adsorption of tetracyclines onto polyethylene microplastics: a combined study of experiment and molecular dynamics simulation. Chemosphere 265:129133, PMID: 33276997, https://doi.org/10.1016/j.chemosphere.2020.129133.
62. Philips LA, Ruffner DB, Cheong FC, Blusewicz JM, Kasimbeg P, Waisi B, et al. 2017. Holographic characterization of contaminants in water: differentiation of suspended particles in heterogeneous dispersions. Water Res 122:431–439, PMID: 28624726, https://doi.org/10.1016/j.watres.2017.06.006.
63. Guo W, Lei L, Shi X, Li R, Wang Q, Han J, et al. 2021. Nonalcoholic fatty liver disease development in zebrafish upon exposure to bis(2-ethylhexyl)-2,3,4,5-tetrabromophthalate, a novel brominated flame retardant. Environ Sci Technol 55(10):6926–6935, PMID: 33938212, https://doi.org/10.1021/acs.est.1c01476.
64. Chen L, Lam JCW, Tang L, Hu C, Liu M, Lam PKS, et al. 2020. Probiotic modulation of lipid metabolism disorders caused by perfluorobutanesulfonate pollution in zebrafish. Environ Sci Technol 54(12):7494–7503, PMID: 32459962, https://doi.org/10.1021/acs.est.0c02345.
65. Kruger NJ. 1994. The Bradford method for protein quantitation. Methods Mol Biol 32:9–15, PMID: 7951753, https://doi.org/10.1385/0-89603-268-X:9.
66. Livak KJ, Schmittgen TD. 2001. Analysis of relative gene expression data using real-time quantitative PCR and the $2^{-\Delta\Delta CT}$ method. Methods 25(4):402–408, PMID: 11846609, https://doi.org/10.1006/meth.2001.1262.
67. Chen J, Ng SM, Chang C, Zhang Z, Bourdon JC, Lane DP, et al. 2009. p53 isoform Δ113p53 is a p53 target gene that antagonizes p53 apoptotic activity via BclxL activation in zebrafish. Genes Dev 23(3):278–290, PMID: 19204115, https://doi.org/10.1101/gad.1761609.
68. Gallo-Oller G, Ordoñez R, Dotor J. 2018. A new background subtraction method for Western blot densitometry band quantification through image analysis software. J Immunol Methods 457:1–5, PMID: 29522776, https://doi.org/10.1016/j.jim.2018.03.004.
69. Carter WO, Narayanan PK, Robinson JP. 1994. Intracellular hydrogen peroxide and superoxide anion detection in endothelial cells. J Leukoc Biol 55(2):253–258, PMID: 8301222, https://doi.org/10.1002/jlb.55.2.253.
70. Qiang L, Cheng J. 2021. Exposure to polystyrene microplastics impairs gonads of zebrafish (*Danio rerio*). Chemosphere 263:128161, PMID: 33297137, https://doi.org/10.1016/j.chemosphere.2020.128161.
71. Zhou W, Tang Y, Du X, Han Y, Shi W, Sun S, et al. 2021. Fine polystyrene microplastics render immune responses more vulnerable to two veterinary antibiotics in a bivalve species. Mar Pollut Bull 164:111995, PMID: 33493858, https://doi.org/10.1016/j.marpolbul.2021.111995.

72. Yin Z, Gong Y, Liu Y, He Y, Yao C, Huang W, et al. 2022. Fucoidan improves growth, digestive tract maturation, and gut microbiota in large yellow croaker (*Larimichthys crocea*) larvae. Nutrients 14(21):4504, PMID: 36364770, https://doi.org/10.3390/nu14214504.
73. Edgar RC. 2013. UPARSE: highly accurate OTU sequences from microbial amplicon reads. Nat Methods 10(10):996–998, PMID: 23955772, https://doi.org/10.1038/nmeth.2604.
74. Magne F, Gotteland M, Gauthier L, Zazueta A, Pesoa S, Navarrete P, et al. 2020. The Firmicutes/Bacteroidetes ratio: a relevant marker of gut dysbiosis in obese patients? Nutrients 12(5):1474, PMID: 32438689, https://doi.org/10.3390/nu12051474.
75. Kan H, Zhao F, Zhang XX, Ren H, Gao S. 2015. Correlations of gut microbial community shift with hepatic damage and growth inhibition of *Carassius auratus* induced by pentachlorophenol exposure. Environ Sci Technol 49(19):11894–11902, PMID: 26378342, https://doi.org/10.1021/acs.est.5b02990.
76. Zhou L, Limbu SM, Shen M, Zhai W, Qiao F, He A, et al. 2018. Environmental concentrations of antibiotics impair zebrafish gut health. Environ Pollut 235:245–254, PMID: 29291524, https://doi.org/10.1016/j.envpol.2017.12.073.
77. Qiao R, Deng Y, Zhang S, Wolosker MB, Zhu Q, Ren H, et al. 2019. Accumulation of different shapes of microplastics initiates intestinal injury and gut microbiota dysbiosis in the gut of zebrafish. Chemosphere 236:124334, PMID: 31310986, https://doi.org/10.1016/j.chemosphere.2019.07.065.
78. Yang LL, Wang GQ, Yang LM, Huang ZB, Zhang WQ, Yu LZ. 2014. Endotoxin molecule lipopolysaccharide-induced zebrafish inflammation model: a novel screening method for anti-inflammatory drugs. Molecules 19(2):2390–2409, PMID: 24566310, https://doi.org/10.3390/molecules19022390.
79. Gao Y, Hou L, Wang Y, Guo S, Yuan D, Jiang Y, et al. 2020. Octreotide alleviates pancreatic damage caused by paraquat in rats by reducing inflammatory responses and oxidative stress. Environ Toxicol Pharmacol 80:103456, PMID: 32673753, https://doi.org/10.1016/j.etap.2020.103456.
80. Wree A, Broderick L, Canbay A, Hoffman HM, Feldstein AE. 2013. From NAFLD to NASH to cirrhosis—new insights into disease mechanisms. Nat Rev Gastroenterol Hepatol 10(11):627–636, PMID: 23958599, https://doi.org/10.1038/nrgastro.2013.149.
81. Sumida Y, Yoneda M. 2018. Current and future pharmacological therapies for NAFLD/NASH. J Gastroenterol 53(3):362–376, PMID: 29247356, https://doi.org/10.1007/s00535-017-1415-1.
82. Arrese M, Cabrera D, Kalergis AM, Feldstein AE. 2016. Innate immunity and inflammation in NAFLD/NASH. Dig Dis Sci 61(5):1294–1303, PMID: 26841783, https://doi.org/10.1007/s10620-016-4049-x.
83. Kumar S, Duan Q, Wu R, Harris EN, Su Q. 2021. Pathophysiological communication between hepatocytes and non-parenchymal cells in liver injury from NAFLD to liver fibrosis. Adv Drug Deliv Rev 176:113869, PMID: 34280515, https://doi.org/10.1016/j.addr.2021.113869.
84. Traussnigg S, Kienbacher C, Halilbasic E, Rechling C, Kazemi-Shirazi L, Hofer H, et al. 2015. Challenges and management of liver cirrhosis: practical issues in the therapy of patients with cirrhosis due to NAFLD and NASH. Dig Dis 33(4):598–607, PMID: 26159280, https://doi.org/10.1159/000375353.
85. Hersoug LG, Møller P, Loft S. 2016. Gut microbiota-derived lipopolysaccharide uptake and trafficking to adipose tissue: implications for inflammation and obesity. Obes Rev 17(4):297–312, PMID: 26712364, https://doi.org/10.1111/obr.12370.
86. Di Lorenzo F, De Castro C, Silipo A, Molinaro A. 2019. Lipopolysaccharide structures of Gram-negative populations in the gut microbiota and effects on host interactions. FEMS Microbiol Rev 43(3):257–272, PMID: 30649292, https://doi.org/10.1093/femsre/fuz002.
87. Luo T, Wang X, Jin Y. 2021. Low concentrations of imidacloprid exposure induced gut toxicity in adult zebrafish (*Danio rerio*). Comp Biochem Physiol C Toxicol Pharmacol 241:108972, PMID: 33418081, https://doi.org/10.1016/j.cbpc.2020.108972.
88. Bhatia S, Prabhu PN, Benefiel AC, Miller MJ, Chow J, Davis SR, et al. 2015. Galacto-oligosaccharides may directly enhance intestinal barrier function through the modulation of goblet cells. Mol Nutr Food Res 59(3):566–573, PMID: 25421108, https://doi.org/10.1002/mnfr.201400639.
89. McCauley HA, Guasch G. 2015. Three cheers for the goblet cell: maintaining homeostasis in mucosal epithelia. Trends Mol Med 21(8):492–503, PMID: 26144290, https://doi.org/10.1016/j.molmed.2015.06.003.
90. Jirillo E, Caccavo D, Magrone T, Piccigallo E, Amati L, Lembo A, et al. 2002. The role of the liver in the response to LPS: experimental and clinical findings. J Endotoxin Res 8(5):319–327, PMID: 12537690, https://doi.org/10.1177/09680519020080050501.
91. Lai Y, Zhou C, Huang P, Dong Z, Mo C, Xie L, et al. 2018. Polydatin alleviated alcoholic liver injury in zebrafish larvae through ameliorating lipid metabolism and oxidative stress. J Pharmacol Sci 138(1):46–53, PMID: 30245287, https://doi.org/10.1016/j.jphs.2018.08.007.
92. Pan YX, Luo Z, Zhuo MQ, Wei CC, Chen GH, Song YF. 2018. Oxidative stress and mitochondrial dysfunction mediated Cd-induced hepatic lipid accumulation in zebrafish *Danio rerio*. Aquat Toxicol 199:12–20, PMID: 29604498, https://doi.org/10.1016/j.aquatox.2018.03.017.
93. Zhao F, Guo M, Zhang M, Duan M, Zheng J, Liu Y, et al. 2022. Sub-lethal concentration of metamifop exposure impair gut health of zebrafish (*Danio rerio*). Chemosphere 303(pt 2):135081, PMID: 35636611, https://doi.org/10.1016/j.chemosphere.2022.135081.
94. Hotamisligil GS, Arner P, Caro JF, Atkinson RL, Spiegelman BM. 1995. Increased adipose tissue expression of tumor necrosis factor-alpha in human obesity and insulin resistance. J Clin Invest 95(5):2409–2415, PMID: 7738205, https://doi.org/10.1172/JCI117936.
95. Esser N, Legrand-Poels S, Piette J, Scheen AJ, Paquot N. 2014. Inflammation as a link between obesity, metabolic syndrome and type 2 diabetes. Diabetes Res Clin Pract 105(2):141–150, PMID: 24798950, https://doi.org/10.1016/j.diabres.2014.04.006.
96. Kahn SE, Hull RL, Utzschneider KM. 2006. Mechanisms linking obesity to insulin resistance and type 2 diabetes. Nature 444(7121):840–846, PMID: 17167471, https://doi.org/10.1038/nature05482.
97. Tanase DM, Gosav EM, Costea CF, Ciocoiu M, Lacatusu CM, Maranduca MA, et al. 2020. The intricate relationship between type 2 diabetes mellitus (T2DM), insulin resistance (IR), and nonalcoholic fatty liver disease (NAFLD). J Diabetes Res 2020:3920196, PMID: 32832560, https://doi.org/10.1155/2020/3920196.
98. Khan RS, Bril F, Cusi K, Newsome PN. 2019. Modulation of insulin resistance in nonalcoholic fatty liver disease. Hepatology 70(2):711–724, PMID: 30556145, https://doi.org/10.1002/hep.30429.
99. Han Y, Zhou W, Tang Y, Shi W, Shao Y, Ren P, et al. 2021. Microplastics aggravate the bioaccumulation of three veterinary antibiotics in the thick shell mussel *Mytilus coruscus* and induce synergistic immunotoxic effects. Sci Total Environ 770:145273, PMID: 33513513, https://doi.org/10.1016/j.scitotenv.2021.145273.
100. Smith M, Love DC, Rochman CM, Neff RA. 2018. Microplastics in seafood and the implications for human health. Curr Environ Health Rep 5(3):375–386, PMID: 30116998, https://doi.org/10.1007/s40572-018-0206-z.
101. Boonsaner M, Hawker DW. 2013. Evaluation of food chain transfer of the antibiotic oxytetracycline and human risk assessment. Chemosphere 93(6):1009–1014, PMID: 23790827, https://doi.org/10.1016/j.chemosphere.2013.05.070.
102. De-la-Torre GE. 2020. Microplastics: an emerging threat to food security and human health. J Food Sci Technol 57(5):1601–1608, PMID: 32327770, https://doi.org/10.1007/s13197-019-04138-1.
103. Wang Y, Zhao X, Zang J, Li Y, Dong X, Jiang F, et al. 2022. Estimates of dietary exposure to antibiotics among a community population in East China. Antibiotics (Basel) 11(3):407, PMID: 35326870, https://doi.org/10.3390/antibiotics11030407.
104. Oliveri Conti G, Ferrante M, Banni M, Favara C, Nicolosi I, Cristaldi A, et al. 2020. Micro- and nano-plastics in edible fruit and vegetables. The first diet risks assessment for the general population. Environ Res 187:109677, PMID: 32454310, https://doi.org/10.1016/j.envres.2020.109677.
105. Li D, Shi Y, Yang L, Xiao L, Kehoe DK, Gun'ko YK, et al. 2020. Microplastic release from the degradation of polypropylene feeding bottles during infant formula preparation. Nat Food 1(11):746–754, https://doi.org/10.1038/s43016-020-00171-y.
106. Food and Agriculture Organization of the United Nations. 2013. FAO Statistical Yearbook. http://www.fao.org/docrep/018/i3107e/i3107e00.htm [accessed 24 December 2021].
107. Barbazuk WB, Korf I, Kadavi C, Heyen J, Tate S, Wun E, et al. 2000. The syntenic relationship of the zebrafish and human genomes. Genome Res 10(9):1351–1358, PMID: 10984453, https://doi.org/10.1101/gr.144700.